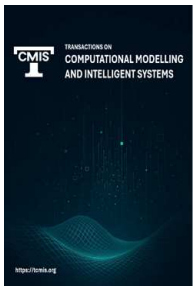

Transactions on
Computational Modeling
and Intelligent Systems

Volume 3, April 2026, Article 10073
https://doi.org/10.65112.tcmis.10073

eISSN: 3108-5202
www.tcmis.org

RESEARCH ARTICLE

Sigmoids based on Mittag-Leffler functions: Ideas, modeling, and computational experiments

Jordan Hristov[1,*]

[1] *Department of Chemical Engineering, University of Chemical Technology and Metallurgy, Sofia, Bulgaria.*
[*] *Corresponding Author. Email: jyh@uctm.edu, jordan.hristov@mail.bg (J. Hristov)*

Article Information

Received: 24 February 2026
Accepted: 7 April 2026
Published 13 April 2026

AMS Classification:
26A33, 34A08

Abstract

Progress has been made in developing sigmoids derived from the Mittag-Leffler function. Generally, the Mittag-Leffler functions of one and two parameters, as well as the Atangana-Baleanu formulation, are used to substitute the traditional exponential in the Verhulst model. Sigmoid formulations have been successfully demonstrated using numerous subcases of the Mittag-Leffler function. Maple and Mathematica computing have enabled us to successfully visualize the results and identify emerging computational problems.

Keywords: Sigmoidal curves, logistic models, Mittag-Leffler functions, fractional derivatives

Contents

1. Introduction

Since the seminal paper by Verhulst in 1845 [1], *logistic* (generally *sigmoid*) functions

$$\frac{dy}{dz} = ry\left(1-y\right) \Rightarrow y = \frac{1}{1+e^{-rz}}, \quad z > 0 \tag{1}$$

have been widely employed in many different domains to describe self-limited population expansion.

Beyond typical growth problems, the fascinating characteristics of logistic functions enable the modeling of many dynamic processes, helping fit curves to experimental data [2, 3] and be key components of neurocomputing as activation functions [4–6]. Numerous improvements and changes have been made during the previous 200 years
[7–10, 35]. For deep and comprehensive analyses of logistic models, we refer to the review in [11] and the recent systematic review [12].

Following the analysis in [12] there are two general trends in improvements of the logistic models :

- Modification of the rate equation, i.e., modifications of the differential equation (the left-hand side of (1) [13–19] by introducing additional parameters and modified birth-death functions.
- Modification of the logistic function [19–27], in a general form

$$y(z) = \frac{1}{1+e^{-rz}} \Rightarrow y(z) = \frac{1}{1+F(z)}, \quad F(z) = f(e^{-z}) \tag{2}$$

the exponential term e^{-rz} is replaced by another function $F\left(z\right)$, based also on the exponential, such that $y\left(z\right)$ obeys the same boundary and initial conditions as the classical logistic model: $y\left(-\infty\right) = 0$, $y\left(\infty\right) = 1$, and $y\left(0\right) = 1/2$.

The present study follows the second trend but, to a greater extent, goes back to the recovery of the governing differential equations, yielding solutions as modified logistic functions; that is, we know the result, with given $F(z)$, and are looking for the modeling equation to which this modification is a solution. This is the general line in this study, but before starting, we have to clear up some details about the existing background, thus allowing us to better present the new results and outline the developments made.

Note: It is important to mention at the beginning that we do not create activation functions [4–6], which in general are simple algebraic expressions, but now we develop a new trend that has never been explored before. Some readers may see activation functions in the results, but this could be a product of their imagination and what they want to see.

1.1. The logistic function overview and key moments

The general expression of the logistic function, for real values of x, is defined as [1]

$$y(x) = \frac{K}{1 + e^{-r(x-x_0)}}, \quad -\infty < x < \infty \tag{3}$$

In (3) K is the carrying capacity, r is the growth rate constant (Malthusian rate constant), while x_0 is x the value at the midpoint where $y(x_0) = K/2$. The logistic function is the solution of a generalized growth modeling equation conceived by Verhulst [1]

$$\frac{dy}{dx} = ry - \phi(y) = ry\left(1 - \frac{y}{K}\right), \quad \phi(y) = y^2, \quad x \geq 0 \tag{4}$$

with initial conditions $y(0) = 1/2$.

The logistic function is symmetrical about the midpoint $x = x_0$ and $y(x_0) = K/2$. It has two asymptotes: $y(+\infty) = K$ and $y(-\infty) = 0$. With $K = 1$, $r = 1$, and $x_0 = 0$ we get

$$y(x) = \frac{1}{1 + e^{-rx}} \tag{5}$$

known as a *sigmoid* (see Remark 2), which is symmetrical and can be presented for $r > 0$ as a growing function, and for $r < 0$ it exhibit a decaying plot symmetrical to that when $r > 0$ (see Figure 1) .

The logistic function is symmetrical, that is $1 - y(x) = y(-x)$, and sometimes

$$^{A}y(x) = 1 - y(x) \tag{6}$$

is termed as an *anti-logistic curve* [28] (we will use this term hereafter (a terminology widely used). It could be considered a complimentary function, too.), that is (see Figure 1). The sum of $y(x)$ and $^{A}y(x)$ is unity, i.e.,

$$y(x) + {}^{A}y(x) = 1 \tag{7}$$

as it follows from their definitions. Moreover, $y(x) - 1/2$ is an odd function, starting at $x = 0$ (we will use the term S-shaped functions in the sequel).

The inverse of the logistic function, the so-called *Logit*, is defined as

$$\text{logit}(y) = y^{-1}(x) = \ln\left(\frac{y}{1-y}\right) \tag{8}$$

The derivative of $y(x) = \frac{e^x}{(1+e^x)^2}$ is bell-shaped , i.e., the Gaussian normal distribution (the blue line in Figure 2), while the undefined integral is $\int \frac{e^x}{1+e^x} = \ln(1 + e^x)$ (the green line in Figure 2).

Remark 1 (On the bell-shaped derivative of the sigmoid function)**.** *We emphasize the importance of the bell-shaped derivative of the sigmoid function because the subsequent examples in this study will include various bell-shaped derivative curves that can be either symmetrical or asymmetrical, depending on the approximation function used in place of the exponential in the logistic law.*

The inflection point is defined by $x = 0$ because

$$\frac{d^2y}{dx^2} = e^x \frac{(e^x - 1)}{(e^x + 1)^2} = 0 \Rightarrow x = 0 \tag{9}$$

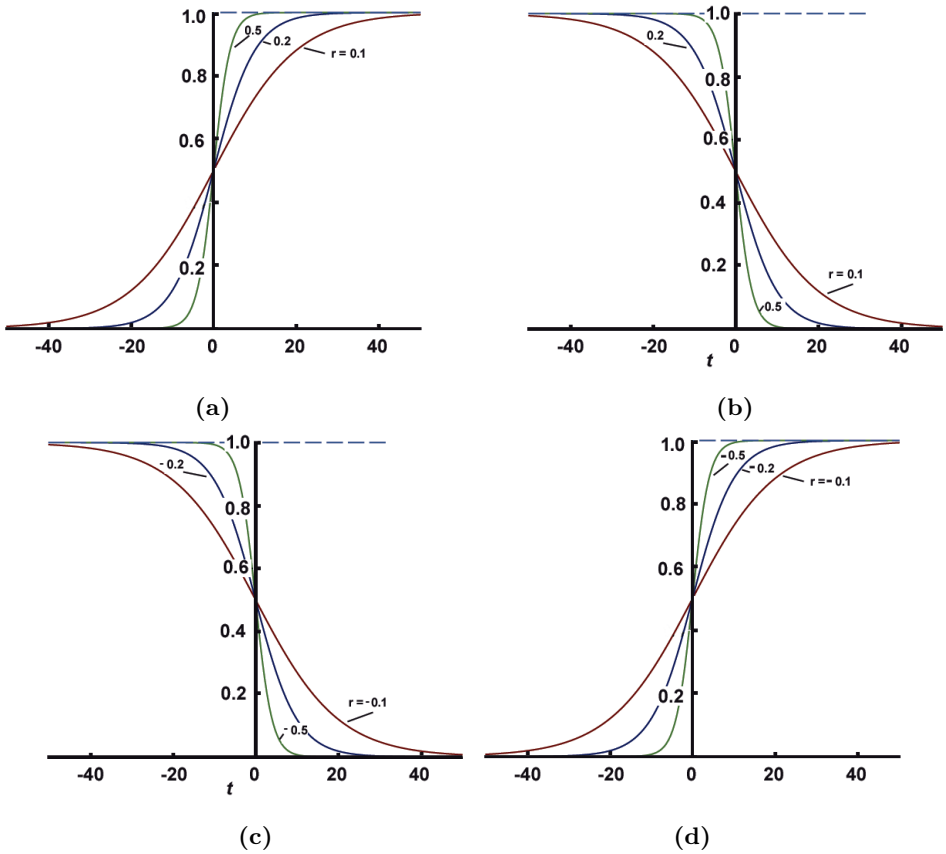

Figure 1. Computer simulations of the sigmoid and anti-sigmoid functions (as a mathematical exercise) for different sign of the rate constant r : (a) and (b) examples for positive r; (c) and (d) examples for positive r.Note: Sigmoids (Left column); Anti-Sigmoids (Right column).

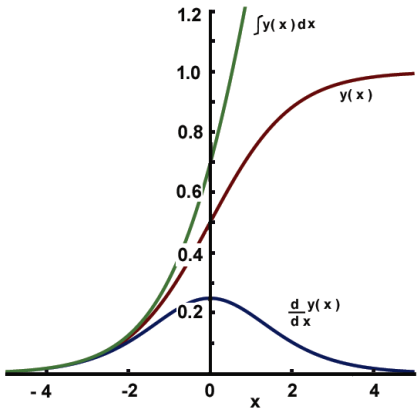

Figure 2. Classical sigmoid function, its derivative and integral.

The Maclaurin series are

$$y(x)=\sum_{n=0}^{\infty}\frac{(-1)^n E_n(0)}{2n!}x^n=\sum_{n=0}^{\infty}\frac{(-1)^{n+1}\left(2^{n+1}-1\right)B_{n+1}}{n=1}x^n=\frac{1}{2}+\frac{x}{4}-\frac{x^3}{48}+\frac{x^5}{480}-\frac{17}{80640}x^{37}\ldots \tag{10}$$

where $E_n(x)$ is the Euler polynomial, and B_n denotes the Bernoulli numbers.

At the end of these introductory notes, we address the logistic regression conceived by Cox [31] in 1958 as a function

$$y = \frac{1}{1+e^{-z}} \tag{11}$$

with $z = \beta_0+\beta_1 x_1+\beta_2 x_2+\ldots \beta_n x_n = ln\frac{y}{1-y}$ a predicted variable probability, where are coefficients of the polynomial approximation in accordance with the Cox regression approach. From (11) we can see that

$$y = \frac{1}{1+e^{-z}} \Rightarrow \frac{1-y}{y} \Rightarrow e^z = \frac{y}{1-y} \tag{12}$$

and therefore, $\ln\left(\frac{y}{1-y}\right) = \beta_0 + \beta_1 x_1 + \beta_2 x_2 + \ldots \beta_n x_n$.

Remark 2 (The logistic function and the sigmoid function: what is the difference?)**.** *Before continuing the study, we have to clarify some points, allowing better distinguishing of the results and how they are related to the existing ones. The sigmoid function and the logistic function are interrelated, but there is a strong hierarchy between them: the logistic function as defined by Eq. (3) is a special case of the sigmoid function (5) (that can be easily obtained from (3) by adequate non-dimensionalization (scaling)—see Section 2.1). Further, the sigmoid function is bounded, i.e., $y(0) = 0$ and $y(\infty) = 1$; in this study we will use a more general term, $S-$ shaped plots or S-curves.*

1.2. The focus of this research, the motivation behind, and its primary approach

The main focus of this study is the generation of logistic functions (13) or sigmoids (S-functions)(14) using the general construction (5), namely

$$y(t) = \frac{1}{1+F(t)}, y(0) = 1/2, y(-\infty) = 0, y(\infty) = 1 \tag{13}$$

$$y(t) = \frac{1}{1+F(t)}, y(0) = 0, y(\infty) = 1 \tag{14}$$

obeying all their properties, but with $F(t)$ not based on the exponential function as in the classical formulation.

Note: The formulations (13) and (14) have equal constructions, but they have different properties depending on the boundary conditions imposed. As a step ahead, and as we will see many examples further in this article, (14) generates S-shaped curves, starting at zero and using mainly $F(t)$ which are unbounded (singular) at the origin, while (13) corresponding to the classical (Verhulst type) logistic behavior, needs $F(t)$ bounded at zero, precisely $F(0) = 1$.

Therefore, the main approach is the so-called "manipulation of the general form of the logistic function" [12] by using functions obeying the same initial and boundary conditions as the exponential function in the classical Verhulst solution [1] so that the output is an S-shaped (sigmoid) function. We are focusing on recovering the modeling equation that the new function may solve; this process can be referred to as "reverse modeling," where the solution is already known, and we need to identify the corresponding equation. As a note clarifying this approach, the first attempt made in this study is to use the Mittag-Leffler function as $F(t)$ as a generalization of the exponential function, a step that has never been applied before.

Note: The suggested *logistic functions* will hereafter be referred to as *sigmoids*. This choice is made for grammatical reasons, to avoid the repeated use of the word "function," and remembering that the exponential in the simplest construction is replaced by various functions obeying certain properties, as it will be explained in detail in the sequel.

1.3. Further text organization

The next part of this article considers: Scaling (Section 2.1) and an unconventional solution of the classical logistic model (Section 2.2), thus allowing us to formulate the main approach applied to all cases discussed after that. The construction of sigmoid models with the Mittag-Leffler function of one parameter is developed in Section 3, with detailed analysis of computation

problems by both Maple and Mathematica. Some subcases related to asymptotics of the Mittag-Leffler function are discussed in Section 3.3 : Sigmoid based on $E_{1/2\,,1}\left(-\tau^{\alpha}\right)$ (Sections 3.3.1 and 3.3.2) and the complimentary error function (Section 3.3.4). Experiments creating sigmoids from the general construction of the Gompertz model, but with the implementation of versions of the Mittag-Leffler function of one parameter, are developed in Section 3.3.5.

Sigmoids based on the Mittag-Leffler function of two parameters are developed in Section 4. General requirements concerning functions that can be used in the construction of sigmoid models are formulated in Section 5.1 in two directions: Functions bounded at the origin (Section 5.2) and unbounded at the origin (Section 5.3), applying the Lambert transform (Section 5.3.1) to the Mittag-Leffler function of one parameter (Section 5.3.2).

An attempt to create sigmoids based on the Mittag-Leffler function of one parameter controlled by a non-integer parameter (Atangana-Baleanu formulation) is developed in Section 6, and a subcase pertinent to the classical logistic function but reformulated in the Caputo-Fabrizio sense (Section 6.2).

The outlines of the main results are discussed in Section 7 with emphasis on model constructions and emerging computational problems.

For creating a well-organized and comprehensive exposition, the auxiliary information is summarized in the Appendices (Section 9).

2. The classic logistic equation: scaling and an instructive solution

Consider the classical Verhulst equation [1] in the form

$$\frac{dy}{dt}=-ry\left(1-y\right) \tag{15}$$

Now, we focus our attention on two steps that underlie the ideas explored in this article:

- The definition of the time scale
- An unconventional solution that draws the route towards the extension of the logistic function and the corresponding models.

2.1. Scaling and time scale

It is well known that the classical formulation of the Verhulst models is

$$\frac{dX}{dt}=rX\left(\frac{K-X}{K}\right)=rX\left(1-\frac{X}{K}\right) \tag{16}$$

where K is the maximum value attained by function $X\left(t\right)$), i.e., the so-called carrying capacity. Defining the dimensionless variable $y=X/K$, where $0<y\leq 1$, we get the form of (15). For the analyses developed in this study, the form (15) is more suitable, as it will be demonstrated in the sequel. From (15) and the well-known solutions (see Appendix A, Section 9.1), the dimension of r is the inverse of time, and in SI units, it is s^{-1}. If we suggest a time scale t_0 such that the dimensionless quantity is defined as $\tau=t/t_0\ \Rightarrow t=\tau t_0$ we may rewrite (15) as

$$\frac{dy}{t_0 d\tau}=-ry\left(1-y\right)\Rightarrow\frac{dy}{d\tau}=-rt_0 y\left(1-y\right)\Rightarrow\frac{dy}{d\tau}=-y\left(1-y\right),\quad t>0,\quad ,\tau=rt>0 \tag{17}$$

If we consider the time scale as $t_0=1/r$, then we get the last dimensionless form of (17). This form is very important for the development of the ideas explored in this article.

Note: The argument t is the so-called *observation time* (with a dimension of s, in contrast to the scaled (dimensionless) time τ). In the further explanations and analyses of the developed solutions, we distinguish both of these definitions. It is important to stress the attention on the possibility to compare many experimental results and their approximation by logistic curves if the argument is $\tau=rt$, rather than when r are different and the argument is the observation time t.

2.2. An unconventional and instructive solution

As a first step let us rearrange the dimensionless (the last one) expression of (17) as

$$\frac{dy}{d\tau} = -y^2\left(\frac{1}{y}-1\right) \Rightarrow \frac{1}{y^2}\frac{dy}{d\tau} = -\left(\frac{1}{y}-1\right) \tag{18}$$

Now, bearing in mind that $\frac{d}{d\tau}\left(\frac{1}{y}\right) = -\frac{1}{y^2}\frac{dy}{d\tau} = -\frac{d}{d\tau}\left(\frac{1}{y}-1\right)$ and denoting $\theta = \left(\frac{1}{y}-1\right)$, we may present the second version of (18) as

$$\frac{d\theta}{d\tau} = -\theta \Rightarrow \theta = C_1\exp\left(-\tau\right) \tag{19}$$

In terms of the original function $y\left(t\right)$ and the observation time t, the solution (19) is

$$\frac{1}{y}-1 = C_1\exp\left(-rt\right) \rightarrow y = \frac{1}{1+C_1\exp\left(-rt\right)} \rightarrow y = \frac{1}{1+C_1\exp\left(-\tau\right)} \tag{20}$$

and for $t=0 \Rightarrow \tau = 0$ it is obvious that $C_1 = 1$.

These solution steps are different from the common ones available in literature (see Appendix A, Section 9.1), and they are instructive in view of the approach applied in this study, when the exponential function in the logistic function is replaced by the Mittag-Leffler version as its generalized version.

Remark 3 (On the solution approach)**.** *The solution approach just demonstrated above touches as ideology the ideas developed by Dattoli and Garra [29] to recover the modeling equation albeit the solution technologies (application of the Laguerre derivative and polynomials [30], and exploring the generalized forms of exponentials) and interpretations of the results are different.*

Remark 4 (On the formulation (20))**.** *The formulation with $C_1 = 1$ is a special case of the general definition of the logistic function and it is symmetrical about the point $(0, 1/2)$, with $y(-\infty) = 0$ and $y(\infty) = 1$.*

Remark 5 (On the rearrangement in (18))**.** *Regarding the right-hand side of the second version of (18) we can see that $(1/y - 1) = (1-y)/y$, which is the formulation of the first step in the logistic regression proposed by Cox [31] (see (11)-(12)), i.e., $e^{-z} = (1-y)/y$, where $z = \beta_0 + \beta_1 x_1 + \beta_2 x_2 + \ldots \beta_n x_n = ln\frac{y}{1-y}$. Thus, the appearance of $(1-y)/y$ is not unusual in the transformation of the logistic model.*

3. Logistic law involving the Mittag-Leffler function of one parameter

3.1. Formulation and governing equation recovery

Let us now consider an extension, practically, an evolution of the logistic law, where the exponential in (20) is replaced by the Mittag-Leffler function of one parameter as its generalization, namely

$$Y_{ML} = \frac{1}{1+C_1E_\alpha\left(-\tau^\alpha\right)}, \quad \tau = rt > 0 \tag{21}$$

and, from $\tau = 0$ it follows that $C_1 = 1$ because for $\tau = 0$ we have $E_\alpha\left(-\tau^\alpha\right)_{\tau=0} = 1$ (i.e.,it is bounded at the origin), and $Y_{ML}\left(\tau = 0\right) = 1/2$.

Now, we are interested in what rate (model) equation could lead to this function as a solution. First, rearrange Eq.(21) as

$$\frac{1}{Y_{ML}} = 1 + E_\alpha\left(-\tau^\alpha\right) \rightarrow \frac{1}{Y_{ML}} - 1 = E_\alpha\left(-\tau^\alpha\right) \tag{22}$$

Then, denoting $\frac{1}{Y_{ML}} - 1 = \frac{1-Y_{ML}}{Y_{ML}} = \Theta\left(\tau\right)$ we have

$$\Theta\left(\tau\right) = E_\alpha\left(-\tau^\alpha\right) \tag{23}$$

Furthermore, we know that $\Theta\left(\tau\right)$ is a solution of the fractional equation (with Caputo derivative)

$$D_\tau^\alpha\Theta\left(\tau\right) = -\Theta\left(\tau\right) \tag{24}$$

Therefore, in terms of what we have

$$D_\tau^\alpha\left(\frac{1-Y_{ML}}{Y_{ML}}\right)=-\left(\frac{1-Y_{ML}}{Y_{ML}}\right) \tag{25}$$

Note: Recall the comments in Remark 5, now related to $1/Y_{ML}-1=\left(1-Y_{ML}\right)/Y_{ML}$, allowing further data fitting through $E_\alpha(-\tau^\alpha)$ such as that in the Cox logistic regression [31] (this problem is beyond the scope of this work).

Without loss of generality, we may replace the function $(1/Y_{ML}\ -1)$ by

$$\Phi(\tau)=Y_{ML}^2\left(\frac{1}{Y_{ML}}-1\right)=Y_{ML}\left(1-Y_{ML}\right)=Y_{ML}^2\Theta(\tau) \tag{26}$$

and after a straightforward rearrangement of equation (25), recalling what we did with the classical logistic equation in Section 2.2, the result is

$$\begin{gathered} D_\tau^\alpha\left(Y_{ML}^2\left(\frac{1}{Y_{ML}}-1\right)\right)=-Y_{ML}^2\left(\frac{1}{Y_{ML}}-1\right)\Rightarrow \\ \Rightarrow D_\tau^\alpha\left(Y_{ML}\left(1-Y_{ML}\right)\right)=-\left(Y_{ML}\left(1-Y_{ML}\right)\right) \end{gathered} \tag{27}$$

For $\alpha=1$ we recover the classic logistic model (15).

Now, applying to both sides of (27) the fractional Riemann-Liouville integral $I_\tau^\alpha f\left(\tau\right)=D_\tau^{1-\alpha}f\left(\tau\right)$ we get

$$\frac{d}{d\tau}\left(Y_{ML}\left(1-Y_{ML}\right)\right)=-\frac{1}{\Gamma\left(\alpha\right)}\int_0^\tau\frac{1}{\left(\tau-s\right)^{1-\alpha}}\left(Y_{ML}\left(s\right)\left(1-Y_{ML}\left(s\right)\right)\right) \tag{28}$$

or simply in terms of $\Phi\left(\tau\right)$ we get a Volterra equation of the first kind

$$\frac{d\Phi\left(t\right)}{d\tau}=-\frac{1}{\Gamma\left(\alpha\right)}\int_0^\tau\frac{1}{\left(\tau-s\right)^{1-\alpha}}\Phi\left(s\right)ds \tag{29}$$

The nonlocal equation in this context, which is a fractional equation, acts as a counterpart to the local Verhulst model. This can be expressed as either (27) or its integral version, (29).

Remark 6 (The data fitting ?: A natural question.)**.** *There is a natural question about whether the data fit the newly formulated logistic model. The answer is straightforward and comes directly from the second version of Eq. (22). The first step is to rearrange the data $Y=Y\left(\alpha,\tau\right)$ as $\left(1-Y\right)/Y=f\left(\alpha,\tau\right)$. Then, $f\left(\alpha,\tau\right)$ has to be fitted by $E_\alpha\left(-\tau^\alpha\right)$ (such comments are made in the final comments of this article, but not developed here). Suggesting this procedure, we have to remember that Y is scaled, that is, $0<Y<1$, so that $\left(1-Y\right)/Y$ is always less than unity and corresponds to the right side of Eq.(22), i.e., $0<E_\alpha\left(-\tau^\alpha\right)\leq1$, which is dimensionless. In this way, all requirements for correct data fitting are satisfied. However, this work addresses the process of the formulation of logistic functions (sigmoids) by the implementation of Mittag-Leffler functions, and the data fitting is not among its tasks; some comments are available in Remark 7, although the data fitting is the next naturally following process that should be resolved.*

3.2. Computations

We will now address computations related to the new logistic function using computer algebra environments of two well-known software packages: Maple and Wolfram Mathematica.

3.2.1. Computations by Maple

In Maple there is no a specific command to calculate the Mittag-Leffler function, in contrast to the $WolframMathematica$ (see Section 3.2.3).

The computations of the new logistic function strongly depends on the accuracy in calculations of the Mittag-Leffler function, precisely its truncated version of the Taylor series expression

$$E_\alpha(-\tau^\alpha)(N) = \sum_k^N \frac{(-1)^k \tau^{\alpha k}}{\Gamma(1+\alpha k)} \tag{30}$$

where N is the number of terms.

The use of the Taylor series expansion invokes two computation problems:

- The required number of terms in the series in view to assure stable behavior of the process.
- The process stability when the argument τ increases beyond certain limits.

Effects of the number of terms in the Mittag-Leffler series at moderate dimensionless times τStarting from $N = 100$ and calculating Y_{ML}, we can see in panels (a), (b), and (c) of Figure 3 that for $\alpha = 0.1$ and $\alpha = 0.2$, there are instabilities and incorrect behavior of the plots. The increase in the number of terms up to $N = 200$ eliminates this effect for the plot corresponding to the case with $\alpha = 0.2$; with $N = 500$, the effect can be eliminated when $\alpha = 0.1$. Hence, expansions with low numbers in the truncated Taylor series ($N < 200$) work well for $\alpha \geq 0.2$, but the decrease in value of α requires more terms; for $\alpha \geq 0.5$ only 100 terms are enough.

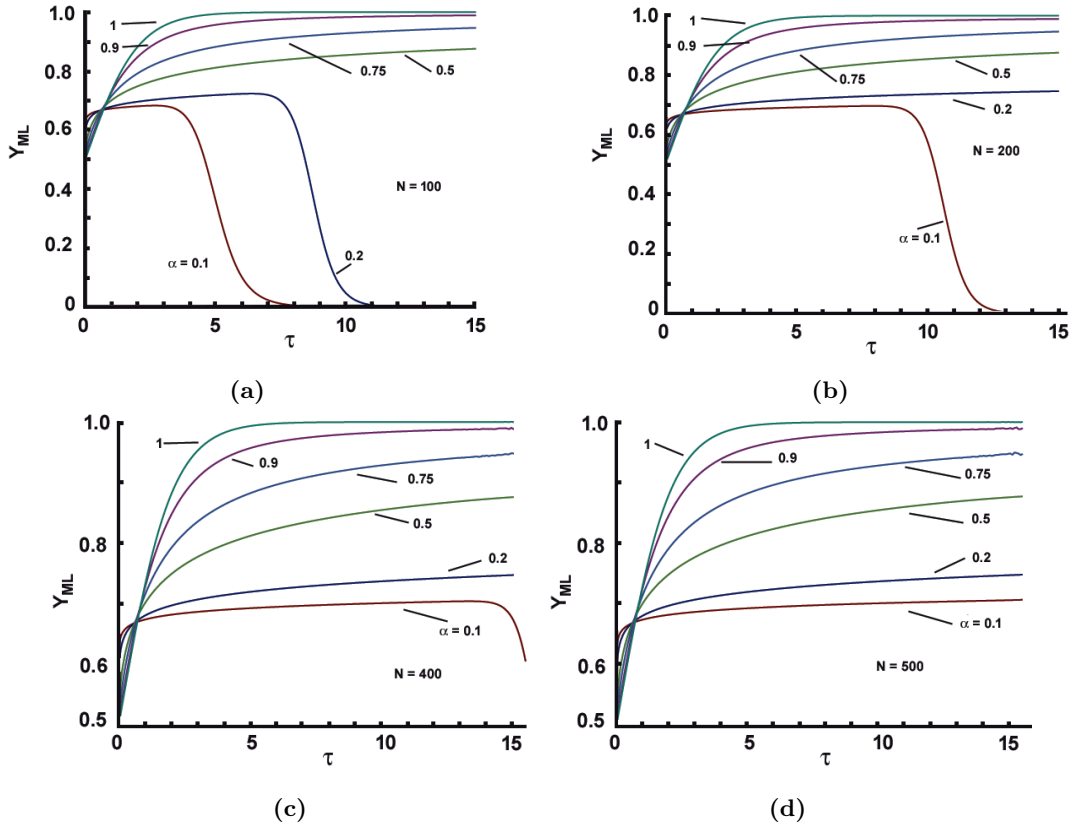

Figure 3. Computer simulations of (21) by Maple for moderate values of the argument τ and different numbers of terms the Mittag-Leffler series, and $0 < \alpha < 1$:(a) $N = 100$, (b) $N = 200$, (c) $N = 400$, (d) $N = 500$

Effects of the increase in the argument τ ***and the terms in the Mittag-Leffler series*** Repeating the same experiments but for $\tau > 15$, we can see in the plots summarized in Figure 4 that there are strong instabilities in all cases, irrespective of the value of α and the number of terms N. Regarding these results, we have to recall that $\tau = rt$ depends on both r and t. To see what the effects are when $\tau \leq 1$, i.e., short dimensionless times, the calculations performed revealed no effect either of the fractional order α or the number of terms N; This can

be attributed to the fact that for $\tau \leq 1$, the Mittag-Leffler function converges rapidly, unlike in cases with larger arguments (larger times). The plots in Figure 5 are obtained with only $N = 35$.

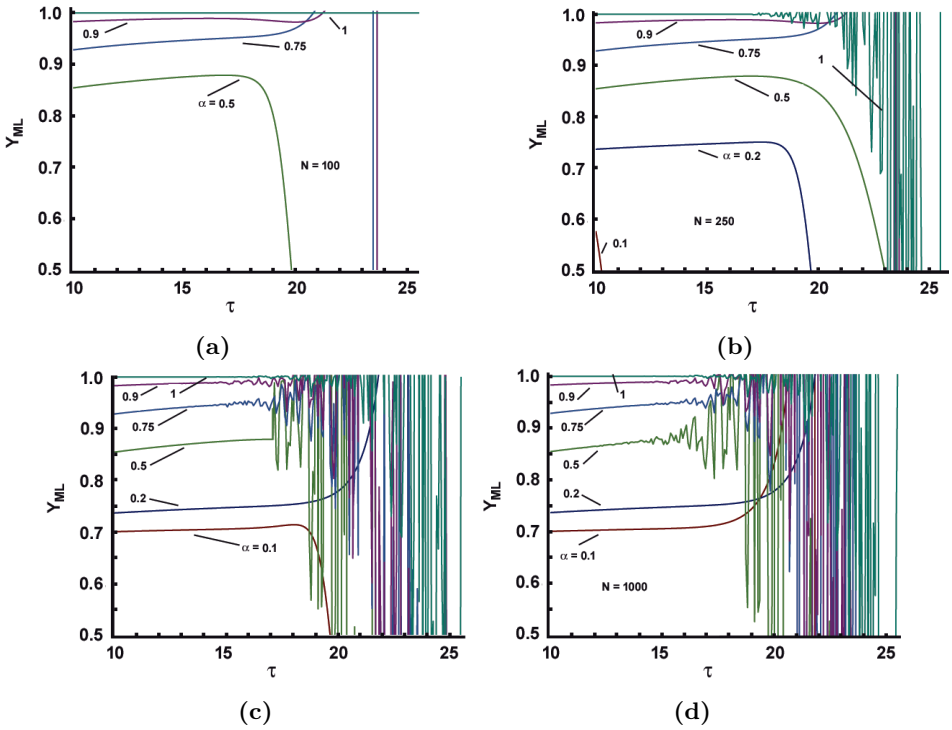

Figure 4. Computer simulations of (21) by Maple: effects of the increase in the argument (the dimensionless time τ) and the number of terms N of the Mittag-Leffler series: (a) $N = 100$, (b) $N = 250$, (c) $N = 500$, (d) $N = 1000$

3.2.2. Cases with asymptotic approximations of the Mittag-Leffler function

Now, we refer to the asymptotic behaviors of the Mittag-Leffler function and the effects on the computation process applying

Asymptotic at the origin $(\tau \to 0^+)$ **:** For $t \to 0^+$ we have (see Eq. (155) in Appendix-B, Section 9.2)

$$Y_{ML(0^+)} = \frac{1}{1 + e^{-\frac{\tau^\alpha}{\Gamma(\alpha+1)}}} \Rightarrow \frac{1 - Y_{ML(0^+)}}{Y_{ML(0^+)}} = e^{-\frac{1}{\Gamma(1-\alpha)}\tau^\alpha} \Rightarrow \ln\left(\frac{1 - Y_{ML(0^+)}}{Y_{ML(0^+)}}\right) = -\frac{1}{\Gamma(1-\alpha)}\tau^\alpha \tag{31}$$

with $\lim_{\tau\to 0^+} Y_{ML}^{0^+} = 1/2$; It can be rearranged as

$$\frac{1 - Y_{ML(0^+)}}{Y_{ML(0^+)}} = e^{-\frac{1}{\Gamma(1-\alpha)}\tau^\alpha} \Rightarrow \ln\left(\frac{1 - Y_{ML(0^+)}}{Y_{ML(0^+)}}\right) = -\frac{1}{\Gamma(1-\alpha)}\tau^\alpha \tag{32}$$

The final form of equation (32) facilitates data fitting in the range as τ approaches 0 (see the comments in Remark 7).

Equation (31), to a greater extent, mimics the solution of the Verhulst model with $r = \frac{1}{\Gamma(\alpha+1)}$, in terms of the observation time t (just replacing t by τ), namely

$$\frac{dY_{ML}^{0^+}}{d\tau} = -\frac{1}{\Gamma(\alpha+1)} Y_{ML}^{0^+}\left(1 - Y_{ML}^{0^+}\right), \quad \tau \geq 0, \quad \tau \to 0^+ \tag{33}$$

Plots of (31) computed by Maple are shown in Figure 5.

Further, comparative calculations of (31) and a truncated Taylor series expansion with $N = 4$ (as suggested by Mathematica-see further the paragraph commenting Eq.(42) in Section 3.2.3)

are shown in Figure 5-panel (b). We can see strong discrepancies for $\alpha < 0.5$ and practically indistinguishable plots beyond this limit (see panel (b) and the augmented section of almost indistinguishable plots in panel (c).

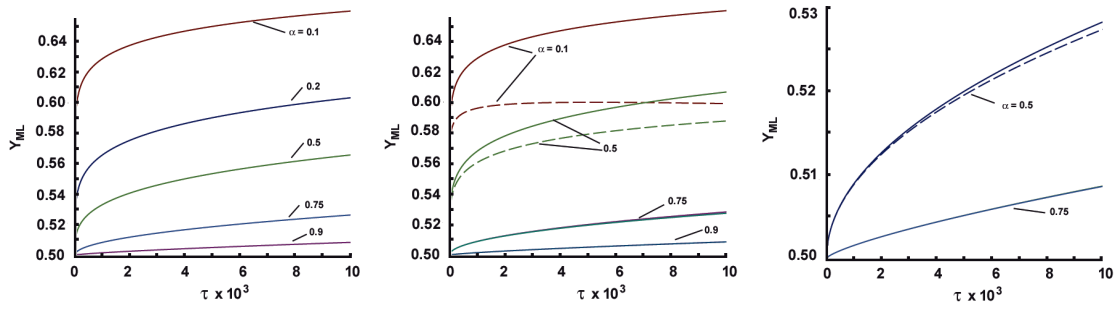

(a) **(b)** **(c)**

Figure 5. Computer simulations by Maple for short dimensionless times: (a) By Mainardi's approximation at the origin of the Mittag-Leffler function (31); (b) A comparison between (31) (solid lines) and the short Taylor series expansion suggested by Mathematica (42)(dashed lines); (c) The same as in (b) for $\alpha = 0.5$ and $\alpha = 0.75$. Note 1: the Mittag-Leffler function was calculated by Maple (Taylor series) with only 4 terms ($N = 4$), to to consistent with the approximation of Mathematica. Note 2: For better graphical presentations the abscissas are presented as $x10^3$, i.e. the mark 2 means 2.10^{-3}.

Approximation at large τ $(\tau \gg 0)$ ***but not*** $\tau \to \infty$ **:** Now, we consider an alternative rational approximation of $E_\alpha\left(-\tau^\alpha\right)$ suggested by Mainardi [32], proved by Simon [33], and discussed by Valerio and Machado [34], that is

$$E_\alpha\left(-\tau^\alpha\right) \approx \frac{1}{1+\tau^\alpha \Gamma\left(1-\alpha\right)}, \quad \tau \gg 0 \tag{34}$$

For $\tau = 0$ we have $E_\alpha\left(0\right) = 1$ and $E_\alpha\left(\infty\right) = 1$, that this intermediate approximation satisfies the main condition imposed on $F\left(\tau\right)$. Its plots, for different values of the parameter α, are shown in Figure 6-panel (a). Thus, the construction of the logistic law is

$$Y_{ML(\tau \gg 0)} = \frac{1}{1+\frac{1}{1+\tau^\alpha \Gamma(1-\alpha)}} \tag{35}$$

The transformation

$$\frac{1-Y_{ML(\tau \gg 0)}}{Y_{ML(\tau \gg 0)}} = \Theta_{ML(\tau \gg 0)} = \frac{1}{1+\tau^\alpha \Gamma\left(1-\alpha\right)} \tag{36}$$

however, does not provide any idea about the governing equation to which $\Theta_{ML(\tau \gg 0)}$ the desired solution is, but allows to be transformed as

$$\frac{2Y_{ML(\tau \gg 0)}-1}{Y_{ML(\tau \gg 0)}} = \tau^\alpha \Gamma\left(1-\alpha\right) \Rightarrow \ln\left(\frac{2Y_{ML(\tau \gg 0)}-1}{Y_{ML(\tau \gg 0)}}\right) = \ln\left(\Gamma\left(1-\alpha\right)\right) + \alpha\tau \tag{37}$$

and to be applied at the initial steps of the data fitting procedure (see Remark 7).

Figure 6-panel (b) reveals stable plots without oscillations as observed in Figure 4, and it is more efficient than the technology with an increase in the number of terms of the truncated series expansion. Besides, to a greater extent, the behavior of the logistic law at $\tau \gg 0$, but not $\tau \to \infty$, resembles that observed when the approximation (38) is applied (see the next paragraph and the plots in Figure 7, because there is an overlapping of the ranges of variations of τ).

Asymptotic at the infinity $\tau \to \infty$ **:** For $t \to \infty$ we have power-law asymptotic of the Mittag-Leffler function (see Eq.(157) in Appendix-B, Section 9.2), so the approximation of the logistic function is

$$Y_{ML}^{\infty} = \frac{1}{1+\frac{\tau^{-\alpha}}{\Gamma(1-\alpha)}}, \quad \tau \geq 0, \quad \tau \to \infty, \quad \lim_{\tau \to \infty} Y_{ML}^{\infty} = 1 \tag{38}$$

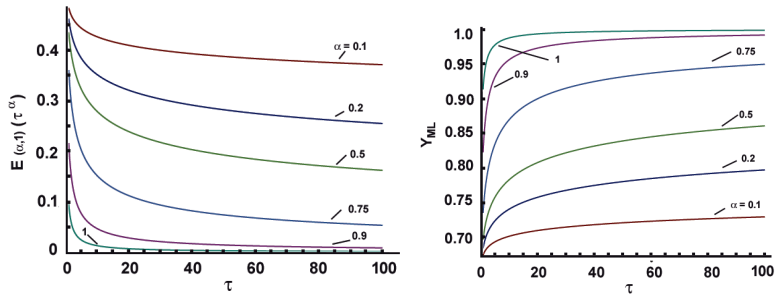

(a) **(b)**

Figure 6. Computer simulations by Maple for large dimensionless times (but not at infinity) for different values of the parameter α: (a) Mittag-Leffler approximation by (34); (b) Logistic functions (35) constructed with the approximation (34).

Now, bearing in mind that is case of the Riemann-Liouville derivative of a constant C we may present (38) as

$$Y_{ML}^{\infty} = \frac{1}{1 + {}^{RL}D_{\tau}^{\alpha} C} \approx 1 \tag{39}$$

The time derivative of (38) is

$$\frac{dY_{ML}^{\infty}}{d\tau} = -\frac{\alpha}{\tau} \frac{\frac{\tau^{-\alpha}}{\Gamma(1-\alpha)}}{\left(1 + \frac{\tau^{-\alpha}}{\Gamma(1-\alpha)}\right)^2}, \quad \tau \to \infty \tag{40}$$

Equation (40), to a greater extent, is like a complex kinetic equation with still unknown physical constitutive equations. Despite this, it is evident that $\frac{dY_{ML}^{\infty}}{d\tau} \to 0$ because the rate of the function approaches zero as it nears the saturation zone $Y_{ML}^{\infty} \to 1$ (see Figures a, b, and c in Figure 7 computed by Maple). The term $\frac{dY_{ML}^{\infty}}{dt}$ represents a time-decaying function, with a decay rate proportional to $\tau^{\alpha+1} \equiv t^{\alpha+1}$, which quickly approaches zero as it is illustrated by the plots in panel d) of Figure 7.

Remark 7 (On the initial steps of data fitting)**.** *The approximations (32) for $\tau \to 0^+$ and (37) for large τ permit making the initial steps in data fitting in these ranges if experimental data exist. Precisely, the exponential approximation (31) or the power law (37) can be used to find some initial information about the value of α and then be used in a more sophisticated data fitting procedure over the entire range of experimental data available.*

3.2.3. Computations by Mathematica

In Wolfram Mathematica, such a flexibility to investigate the effect of the parameters of the Taylor series $E_{\alpha,\beta}(-\tau^{\alpha})$ (two-parameter Mittag-Leffler function) does not exist since there are direct commands for calculations and plotting

$$Series[MittagLefflerE[\alpha, \beta, z], z, z_{min}, z_{max}], \quad Plot[MittagLefflerE[\alpha, \beta, z], z, z_{min}, z_{max}] \tag{41}$$

without any explanations about the intimate moments of the calculation procedure.

The computations (with $E_{\alpha,1}(-\tau^{\alpha})$) illustrated by Figure 8 reveal smooth plots (see Figure 8). In contrast to the computations with Maple, here we have no information about the number of terms used or about any other algorithms used, but we can see very smooth plots generated.

However, if truncated series are used, then the effect of the number of terms is the same as already observed with commutations performed by Maple. Precisely, good sigmoid plots can be obtained with a high number of terms, and this effect is strong when $\alpha < 0.5$, and we can see the effects in Figure 9. The observed calculation problems, irrespective of the computer code used, can be attributed to the slow convergence of the Mittag-Leffler function.

On the asymptotic computations by Mathematica At the Mathematica webpage, the series expansion at the origin is assigned to the command $Series[MittagLefflerE[\alpha, \beta, z], \{z, 0, 4\}]$

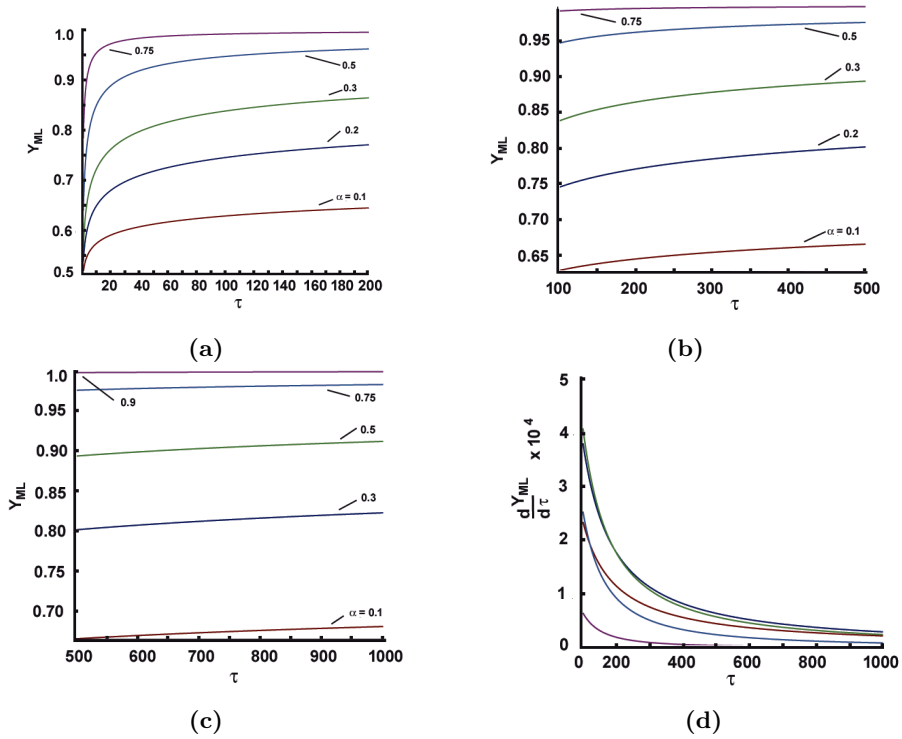

Figure 7. Computer simulations by Maple of (39) for large dimensionless times using the approximation for $\tau \to \infty$. Panels (a), (b) and (c): different time sections, but in all cases large times. (d) The derivative evolution (Eq. (40) for large τ, as in panels (a) and (c). In all cases $N = 400$

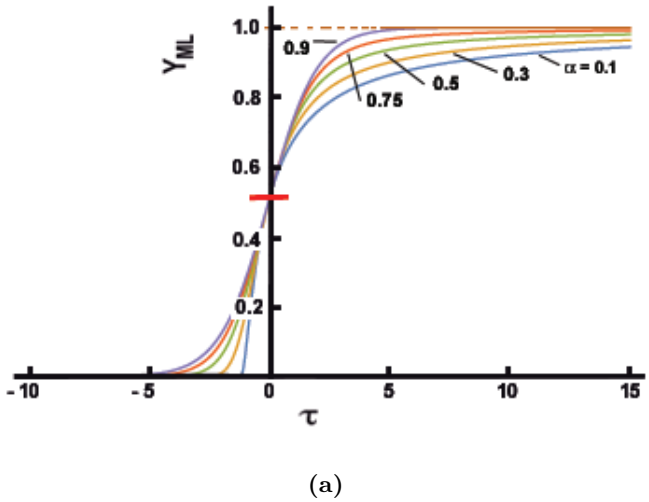

(a)

Figure 8. Computer simulations by Mathematica for different values of the fractional order α for moderate dimensionless times τ using the Mathematica commands in (41)

.

corresponding to the short-term series (in the original notations)

$$\frac{1}{Gamma[\beta]} + \frac{z}{Gamma[\alpha+\beta]} + \frac{z^2}{Gamma[2\alpha+\beta]} + \frac{z^3}{Gamma[3\alpha+\beta]} + \frac{z^4}{Gamma[4\alpha+\beta]} \quad (42)$$

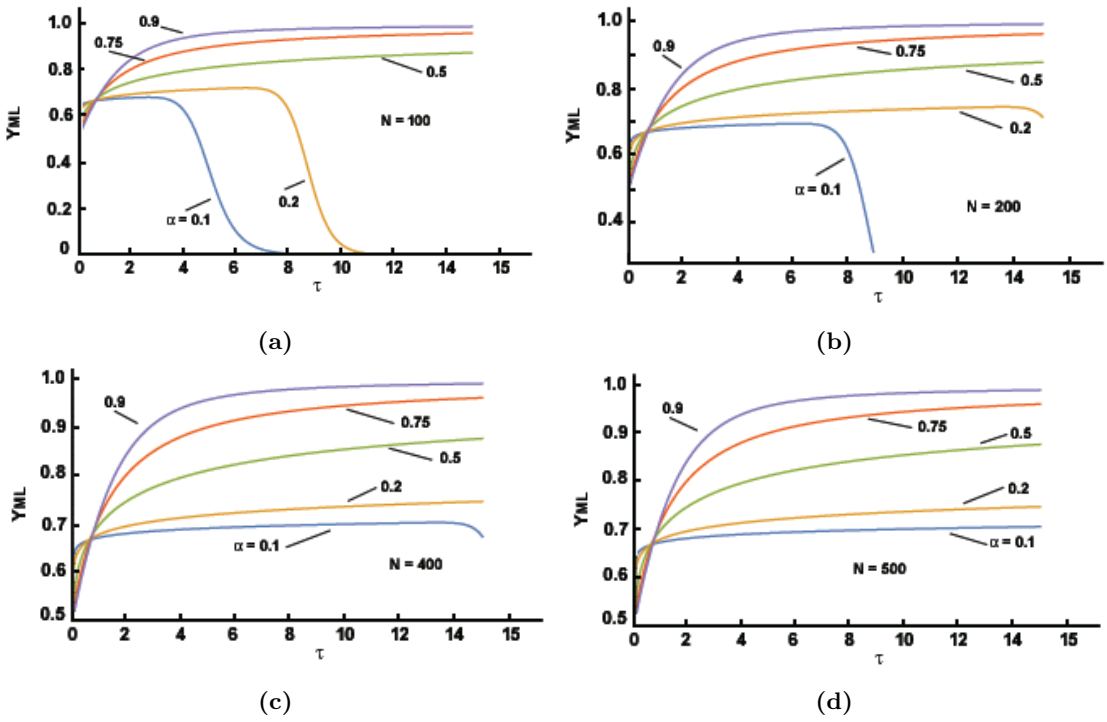

Figure 9. Computer simulations by Mathematica for different values of the fractional order α for moderate dimensionless times τ: Effect the number of term in the truncated Mittag-Leffler. Note: the number of terms for each computation is available in inside the figures.

.

At the infinity, the command is $Series[MittagLefflerE[1, 1/2, z], \{z, \infty, 6\}]//NormalFullSimplify$ corresponding to the approximation

$$e^z\sqrt{z} + \frac{-10395 + 2z(945 + 2z(-105 + 2z(15 - 6z + 4z^2)))}{64\sqrt{\pi}z^6} \tag{43}$$

Note: To calculate what is needed in this study, we have to substitute $z = -\tau^\alpha$ in (42) and compute the short time approximations (see Figure 5-panel (b) and Figure 10-panel (a)). However, for the approximation at infinity, such a substitution is possible, but in the logistic function, it is needed to introduce the function (43) with a negative sign (the computations are illustrated in Figure 10-panels (a) and (b).

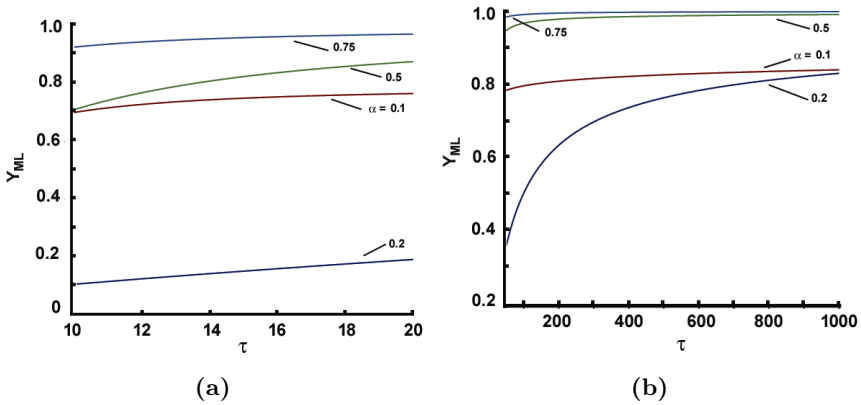

Figure 10. Computer simulations of asymptotic approximations at the infinity by Mathematica for different values of the fractional order α by (43): (a) Moderate long dimensionless times ; (b) Very long dimensionless times

3.2.4. Mittag-Leffler distribution and its sigmoid

Now, let us look back on the formulation (22) and the Mittag-Leffler distribution G_τ^α [36–40] (see Eq.(172)in Appendix B); precisely, Eq. (22) can be reformulated as

$$2-\frac{1}{Y_{ML}}=1-E_\alpha\left(-\tau^\alpha\right)\Rightarrow 2-\frac{1}{Y_{ML}}=G_\tau^\alpha,\quad \tau\geq 0 \tag{44}$$

with $G_\tau^\alpha\left(0\right)=0$ and $G_\tau^\alpha\left(\infty\right)=1$. Differentiating both sides of (44) with respect to τ we get three different forms of an alternative equation related to the generalized formulation of the sigmoid (21), namely

$$\frac{dY_{ML}}{d\tau}=-\frac{dE_\alpha\left(-\tau^\alpha\right)}{d\tau}\Rightarrow\frac{dY_{ML}}{d\tau}=Y_{ML}^2\frac{d}{d\tau}G_\tau^\alpha\Rightarrow\frac{dY_{ML}}{d\tau}=Y_{ML}^2g_\tau^\alpha,\quad \tau\geq 0 \tag{45}$$

To clarify these comments, we show the distribution G_τ^α and its derivative (its density distribution) g_τ^α in Figure 11-panel (a), parallel to the sigmoid defined by Eq.(22) (Figure 11-panel (b)), thus demonstrating their different natures, precisely, the behaviors at the origin.

In addition, based on the properties of the density distribution g_τ^α, we may construct a new sigmoid (see the plots in Figure 11-panel (c).

$$^gY_\tau^\alpha\left(\tau\right)=\frac{1}{1+g_\tau^\alpha\left(\tau\right)},\quad 0<\alpha\leq 1,\quad \tau\geq 0 \tag{46}$$

With $g_\tau^\alpha\left(0^+\right)\to\infty$ and $g_\tau^\alpha\left(\infty\right)\to 0$ we have $^gY_\tau^\alpha\left(0^+\right)=0$ and $^gY_\tau^\alpha\left(\infty\right)\to 1$, respectively. Hence, g_τ^α is unbounded at the origin (see Section 5.3 with such examples) and as a consequence, for $\tau\geq 0$), the sigmoid starts at $^gY_\tau^\alpha(0,0$ in contrast to the case with the model (21) where staring point is $Y_{ML}(0,1/2)$.

Note: Such types of sigmoids, as those based on G_τ^α and the newly defined $^gY_\tau^\alpha\left(\tau\right)$, are further discussed as S-shaped functions, taking into account their common property of starting at $\tau=0$, i.e., the point $(0,0)$, in contrast to the classic logistic law, which starts at the point $(0,1/2\ )$ (see Section 5.3).

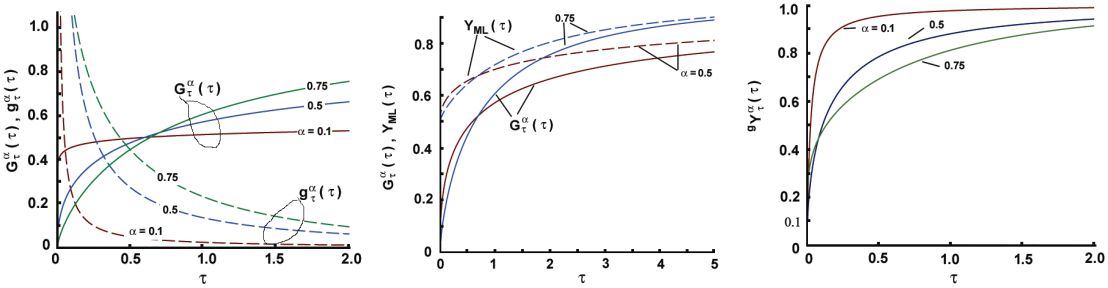

Figure 11. Computer simulation of the Mittag-Leffler distribution and related sigmoids: (a) Mittag-Leffler distribution G_τ^α (CDF) (solid lines) and its derivative (PDF) (dashed lines) for different values of the parameter α. (b) Comparative plots G_τ^α and sigmoids $Y_{ML}(\tau)$(based on $E_\alpha\left(-\tau^\alpha\right)$ (Eq.(21))). (c) Sigmoids $^gY_\tau^\alpha$ (S-shaped curve) based on g_τ^α (unbounded at the origin) at different values of α.

3.3. Sigmoids from some subcases

Now, we consider cases where $E_{\alpha,1}\left(-\tau^\alpha\right)$ can be represented by well-known functions. We have to recall that all these special cases are obtained as approximations when the number of terms in the Taylor series expansion is infinite.

3.3.1. Sigmoids from $E_{1/2\ ,1}\left(-\tau^\alpha\right)$ - Experiment 1

Consider the special case

$$E_{1/2\ ,1}\left(z\right)=e^{z^2}erfc\left(-z\right) \tag{47}$$

where $erfc(z) = 1 - erf(z)$ is the complimentary error function $\frac{2}{\sqrt{\pi}} \int_z^\infty e^{-t^2} dt$.

Note: For $z > 0$, $erfc(z) \approx \frac{1}{6} e^{z^2} + \frac{1}{2}^{\frac{4}{3} z^2}$, and $erf(z) \leq e^{-z^2}$.

For clarity of the calculation results, it is shown in Figure 12-panel (a), parallel to a plot created by the Taylor series expansion

$$E_{1/2,1} \approx \sum_{k=0}^{N} \frac{z^k}{\left(\Gamma \frac{k}{2} + 1\right)} \tag{48}$$

truncated up to $N = 150$ terms; in (47) z should be replaced by $-\tau$ for correct calculations.

The function $E_{1/2\,,1}\left(-\tau^{\alpha}\right)$ is bounded at the origin and vanishes for large τ, thus obeying all properties allowing the construction

$$Y_{ML(1/2,1\,)} = \frac{1}{1 + E_{1/2\,,1}\left(\tau\right)} = \frac{1}{1 + e^{\tau^2} erfc\left(-\tau\right)} \tag{49}$$

to be considered as a sigmoid function, namely: $Y_{ML(1/2,1\,)}\left(0\right) = 1/2$, $Y_{ML(1/2,1\,)}\left(\infty\right) = 1$, as well as $Y_{ML(1/2,1\,)}\left(-\infty\right) = 0$.

Moreover, the sigmoid function (49) is asymmetric with a midpoint at $(0, 1/2\,)$ (see Figure 12-panel (c)). Calculations of $Y_{ML(1/2,1\,)}$ by (49) and when $E_{1/2\,,1}\left(-\tau^{\alpha}\right)$ as a series is used, this results in different plots, which is a natural result because we use a truncated series (Eq. (47) as an approximation when $N \to \infty$).

If we consider $Y_{ML(1/2,1\,)}$ as a cumulative distribution function (CDF), then we see that it is asymmetric but satisfies the boundary conditions $Y_{ML(1/2,1\,)}\left(-\infty\right) = 0$ and $Y_{ML(1/2,1\,)}\left(\infty\right) = 1$.

From this point of view, the corresponding probability density function (PDF) is $\frac{dY_{ML(1/2,1\,)}}{d\tau}$ is a bell-shaped, asymmetric, and shifted to the left (see Figure 12-panel (d))

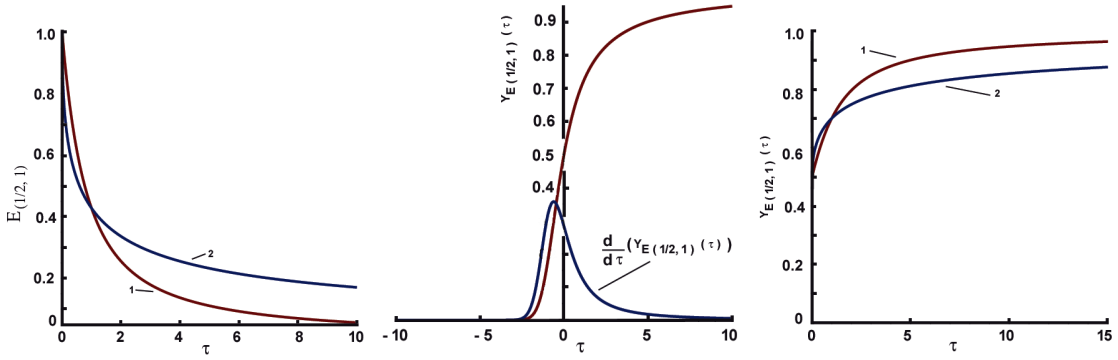

(a) **(b)** **(c)**

Figure 12. Simulations (by Maple) of $E_{1/2,1}(-\tau^{\alpha})$ and the resultant sigmoid $Y_{ML1/2,1}$: (a) The function $E_{1/2,1}$ calculated by (47)-line 1 (red color online) and a truncated series expansion ($N = 150$)-line 2 (blue color online). (b) A non-symmetric sigmoid function generated by (49)(red color online), considered as CDF, and its derivative considered as PDF. (c) Sigmoid functions for $\tau > 0$, using (49)-line 1 (red color online) and a truncated series expansion-line 2 (blue color online).

3.3.2. *Sigmoids from* $E_{1/2\,,1}\left(\tau^{\alpha}\right)$ *- Experiment 2:*

Let us suggest that we may construct the sigmoid-type function

$${}^{R}Y_{1/2,1}\ \left(\tau\right) = \frac{1}{1 + \frac{1}{E_{1/2,1}\left(\tau\right)}} \tag{50}$$

That is, our function $F(\tau)$ is $F(\tau) = \left(E_{1/2}, 1\right)^{-1} = \left(e^{\tau^2} erfc(-\tau)\right)^{-1}$. As a result, we have two cases:

- Case with $E_{1/2\ ,1}$, and then the sigmoid-like function is

$$ {}^{R}Y^{+}_{1/2,1}(\tau) = \frac{1}{1+\frac{1}{E_{1/2,1}(\tau)}} \tag{51} $$

In this case, we have ${}^{R}Y^{+}_{1/2,1}(-\infty) \to 0$, ${}^{R}Y^{+}_{1/2,1}(+\infty) \to 1$, ${}^{R}Y^{+}_{1/2,1}(0) = 1/2$, and the logistic plot is strongly asymmetric; The derivative $\frac{d}{d\tau}{}^{R}Y^{+}_{1/2,1}(\tau)$ is bell-shaped and asymmetric with a long decaying tail towards $\tau \to -\infty$, while for $\tau \to +\infty$ it vanishes rapidly. All these functions are shown in Figure 13-panel (a).

Additional experiments performed by Mathematica are shown in Figure 14, and there is no detectable difference with respect to the plots generated by Maple (see figures (a) and (b)). However, an attempt to use the truncated series (48) reveals that there is a strong effect of the number of terms included in the calculations, the same problem discussed earlier when Maple was used for simulations.

- Case with $E_{1/2,1}(-\tau)$: With $E_{1/2,1}(-\tau)$ we have a possibility to construct a sigmoid-like function (Figure 13-panel (b))

$$ {}^{R}Y^{-}_{1/2,1}(-\tau) = \frac{1}{1+\frac{1}{E_{1/2,1}(-\tau)}} \tag{52} $$

With ${}^{R}Y^{-}_{1/2,1}(-\infty) \to 1$, ${}^{R}Y^{-}_{1/2,1}(+\infty) \to 0$, ${}^{R}Y^{-}_{1/2,1}(0) = 1/2$, but in this case $\frac{d}{d\tau}{}^{R}Y^{-}_{1/2,1}(-\tau) < 0$ in the entire range of variations of τ.

Hence, we got two sigmoid-like functions, both of them asymmetrical with respect to the origin.

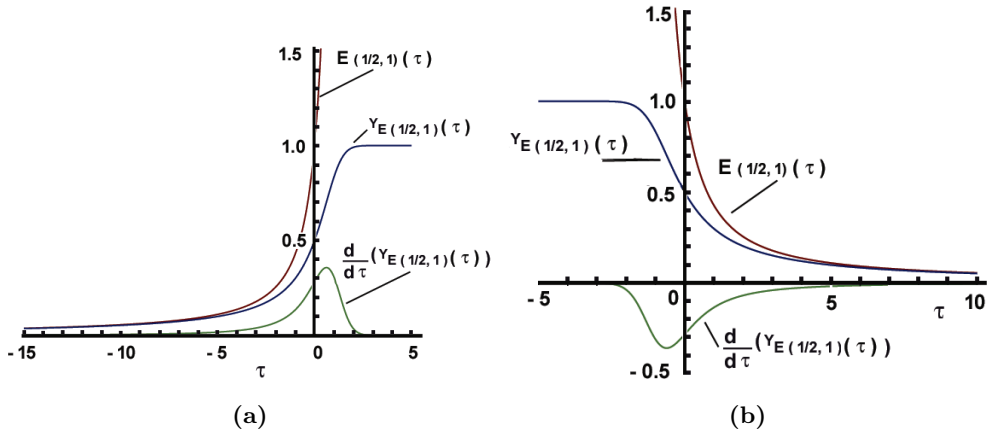

Figure 13. Sigmoid-type functions generated by $E_{1/2,1}(\tau)$: Experiment-2. Simulations (by Maple): (a) Case 1. (b) Case 2.

3.3.3. Case with a sigmoid derived from $E_{1/2,1}\left(\tau^{1/2}\right)$ - Experiment 3

With $F(\tau) = E_{1/2,1}\left(\tau^{1/2}\right)$ defined as

$$ E_{1/2}\left(-\tau^{1/2}\right) = e^{\tau}\left[1+erf\left(\tau^{1/2}\right)\right]e^{\tau}erf\left(-\tau^{1/2}\right), \quad \tau \in \mathbb{C} \tag{53} $$

we can formulate a sigmoid function (see the plots in Figure 15-panel (a) and the inset)

$$ Y_{1/2,1}\left(\tau^{1/2}\right) = \frac{1}{1+E_{1/2}\left(-\tau^{1/2}\right)} \tag{54} $$

For $\tau \to \infty$ we have $Y_{1/2,1}(+\infty) = 1$ because $E_{1/2}\left(-\tau^{1/2}\right)(\tau \to \infty) = 0$. However, $Y_{1/2,1}\left(\tau^{1/\,2}\right)$ is non-normalized for $\tau \geq 0$ having an asymmetric derivative, and for $\tau \to 0$ we get $Y_{1/2,1}(0) = 0.843$. The normalized sigmoid is (see such rescaling procedures in the next sections 3.3.4 and

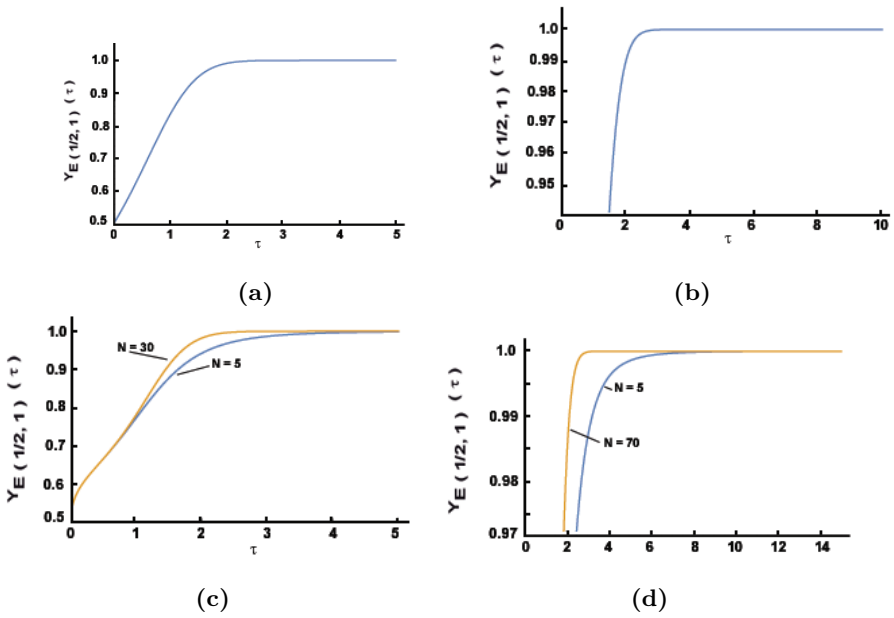

Figure 14. Simulations by Mathematica of the sigmoid $Y_{E1/2,1}$ using Eq.(50): (a) With the $Erfc[x]$ function for small τ. (b) With the command function $Series[MittagLefflerE[1/2,1,\tau],\{\tau,0,10\}$ for large τ. (c) and (d) Simulations by truncated series (see Eq. (48)) and effects of the number of terms N.

3.3.5)

$$\bar{Y}_{1/2,1}\left(\tau^{1/2}\right)=\frac{Y_{1/2,1}\left(\tau^{1/2}\right)-B}{1-B},\quad B=0.843 \tag{55}$$

Now $\bar{Y}_{1/2,1}\left(0\right)=0$ and $\bar{Y}_{1/2,1}\left(\infty\right)=1$ (see Figure 15-panel (c)) obey the general sigmoid properties.

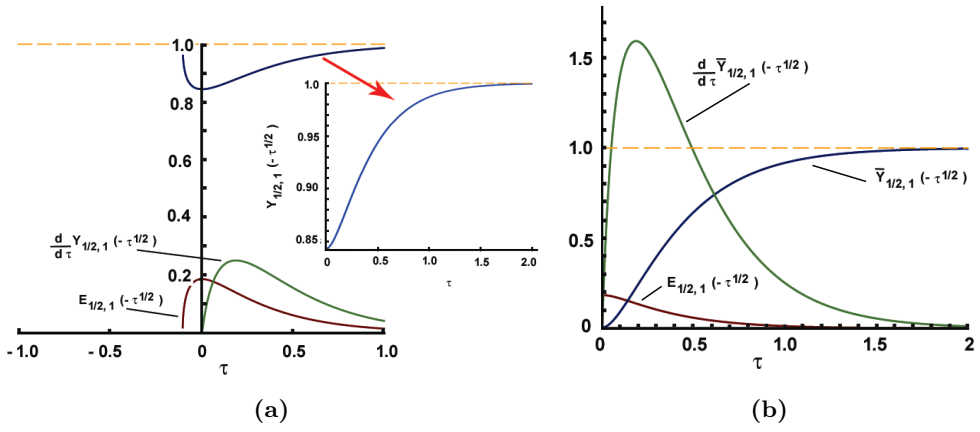

Figure 15. Sigmoid generated by $E_{1/2,1}(-\tau^{1/2})$ (Simulations (by Maple): (a) $E_{1/2,1}(-\tau^{1/2})$, the non-normalized sigmoid and its derivative (Inset: an augmented section of the non-normalized sigmoid) (b) Normalized sigmoid $\bar{Y}_1/2,1(-\tau^{1/2})$ and its derivative.

3.3.4. A sigmoid based on the complimentary error function - Experiment 4

The error function is a specific type of confluent hypergeometric function and can be expressed as a special case of the Mittag-Leffler function of one parameter, precisely $E_{1/2,1}\left(z^2\right)=erf\left(z\right)$ (see additional details in Remark 8). Its plot resembles a logistic one (see Figure 16-panel (a)),

but the saturation (i.e., the limit $\to 1$) is reached for $z<0$, while the decrease for $z>0$ is rapid to zero.

As an experiment, we construct

$$Y_{erfc}(z)=\frac{1}{1+erfc(z)}=\frac{1}{1+(1-erf(z))}=\frac{1}{2-erf(z)} \tag{56}$$

Now, $Y_{erfc}(-\infty)\to 1/3$, $Y_{erfc}(\infty)\to 1$, and $Y_{erfc}(0)\to 1/2$, because $erf(0)=0$, $erf(-\infty)=-1$, $erf(\infty)=1$. Further, we have

$$\frac{1}{Y_{erfc}(z)}=1+erfc(z)=1-erf(z) \tag{57}$$

Taking into account that $\frac{d}{dz}erf(z)=\frac{2}{\sqrt{\pi}}e^{-z^2}$, and differencing both cites of (57), we get

$$\frac{dY_{erfc}}{dz}=Y_{erfc}^2\frac{4}{\sqrt{\pi}}e^{-z^2}=\frac{4}{\sqrt{\pi}}e^{-z^2}\frac{1}{(1+erfc(z))^2} \tag{58}$$

Now, let us consider (56) as a cumulative distribution function (CDF) and (58) as its probability density function (PDF): The CDF exhibits two saturation levels: $Y_{erfc}(+\infty)\to 1$ and $Y_{erfc}(-\infty)\to 1/3$, and the PDF is bell-shaped and slightly shifted to the right. However, we see from Figure 16-panel (b) that not all conditions to accept (56) as CDF are obeyed; precisely $Y_{erfc}(+\infty)\to 1$, but $Y_{erfc}(-\infty)\to 1/3$ instead of the correct requirement $Y_{erfc}(-\infty)\to 0$ levels. We can correct this, i.e., normalize the distribution, by a shifting procedure as

$$\bar{Y}_{erfc}=\frac{Y_{erfc}-1/3}{1-1/3}=\frac{1}{2}\left(\frac{3}{1+erfc(z)}-1\right),\quad \frac{d\bar{Y}_{erfc}}{dz}=\frac{3}{\sqrt{\pi}}\frac{e^{-z^2}}{(1+erfc(z))^2} \tag{59}$$
$$\bar{Y}_{erfc}(-\infty)=0,\quad \bar{Y}_{erfc}(+\infty)=1$$

and the normalized version is shown in 16-panel (c); The same calculations done by Mathematica and the resultants are shown in Figure 17 showing almost identical plots.

Remark 8 (The complimentary error function: some details)**.** *The complementary error function $erfc(z)$ is related to the Gaussian error function $erf(z)$ as $erfc(z)=1-erf(z)$, where the integral version and Maclaurin series of $erf(z)$ and $erfc(z)$ are*

$$erf(z)=\frac{2}{\sqrt{\pi}}\int_0^z e^{-t^2}dt=\frac{2}{\sqrt{\pi}}\sum_{k=0}^{\infty}\frac{(-1)^k z^{2k+1}}{k!\,(2k+1)},\quad erfc=\frac{2}{\sqrt{\pi}}\int_z^{\infty}e^{-t^2}dt \tag{60}$$

or through the incomplete Gamma function as $erf(z)=\left(\Gamma\frac{1}{2},z^2\right)$. Moreover, $erf(z)$ is symmetrical about the vertical axis (odd function), i.e., $erf(-z)=-erf(z)$ and $erfc(-z)=2-erfc(z)$.

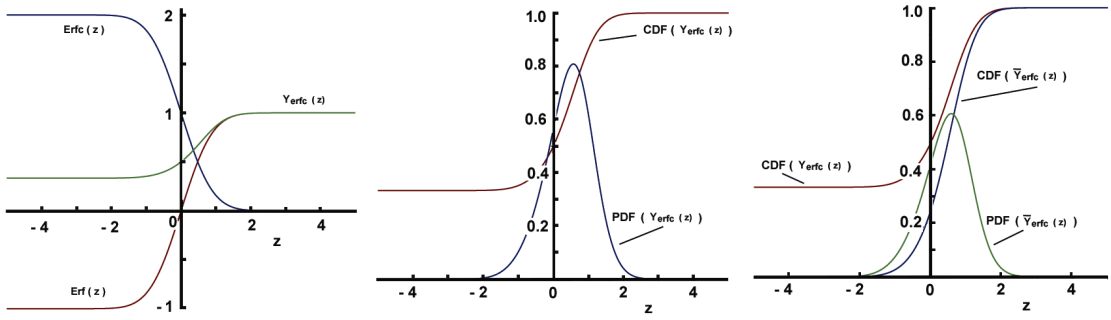

(a) **(b)** **(c)**

Figure 16. Simulations by Maple: (a) Error function (*erf*) (red color online), the complimentary error function (*erfc*) (blue color online) and the logistic function Y_{erfc} (green color online). (b) The logistic function Y_{erfc} as CDF (red color online) and its PDF (blue color online). (c) The logistic function Y_{erfc} (red color online) and its normalized CDF (blue color online) and PDF (green color online).

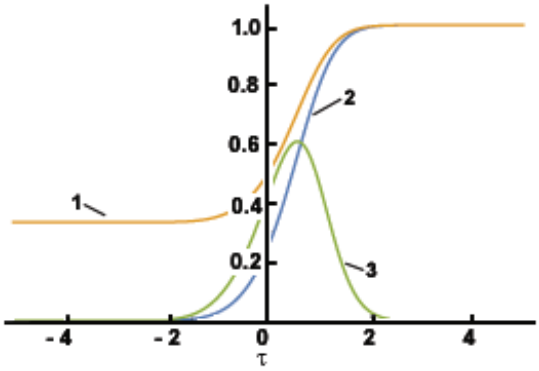

(a)

Figure 17. Simulation by Mathematica (as in Figure 16)-(c): 1-The generated logistic curve (CDF), 2-Rescaled, 3-The derivative (PDF)

3.3.5. Gompertz-like sigmoids with $Erf(\tau)$ and $Erfc(\tau)$: Experiments

The classic Gompertz sigmoid: The Gompertz sigmoid [9,35] is defined as

$$^{G}Y = Ae^{-be^{-ct}}, \quad \tau \geq 0 \tag{61}$$

This function is an asymmetric sigmoid that strongly depends on the values of the coefficients; an example is shown in Figure 18. Now, we consider variations of the Gompertz sigmoid, generally defined as

$$^{G}Y = AF_1\left[F_2\left(\tau\right)\right], \quad \tau \geq 0 \tag{62}$$

where, in the classical formulation (61): $F_2\left(x\right) = ke^{-cx}$ and $F_1\left(x\right) = Ae^{-bF_2(x)}$.

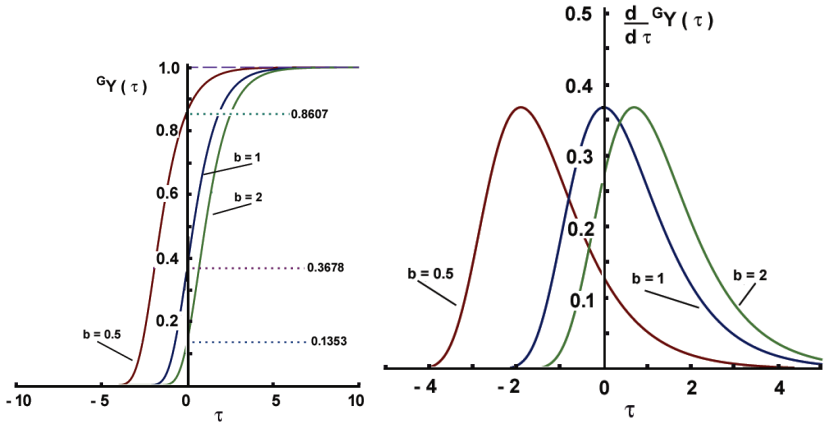

(a) **(b)**

Figure 18. Gompertz sigmoid in three case with different values of the coefficient b: (a) Sigmoids (the dotted lines mark the point $^{G}Y(0)$. (b) The derivatives of the sigmoids presented in panel (a).

Sigmoid with $F_1 = Erf\left(\tau\right)$ ***and*** $F_2 = Erfc\left(\tau\right)$. Let us define the sigmoid as

$$^{G}Y_1 = 1 - A_1 Erfc\left[-b_1 Erf\left(-\tau\right)\right] \tag{63}$$

$$\frac{d^{G}Y_1}{d\tau} = \frac{4}{\pi}e^{-erf(x^2)}e^{-x^2} = \frac{4}{\pi}e^{-\left[erf(x^2)+x^2\right]} \tag{64}$$

The plots in Figure 19 (with $k = A_1 = b_1 = 1$, for the sake of simplicity) reveal a symmetric sigmoid passing through $\tau = 0$, but with saturation at about $^{G}Y_1\left(\infty\right) = 0.8$ (see Figure 19-panel (a), and a symmetric bell-shaped derivatives (Figure 19-panel (b)).

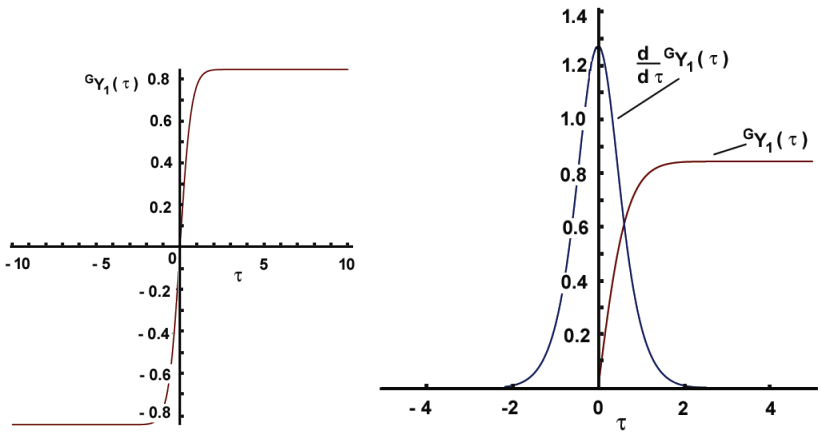

(a) **(b)**

Figure 19. Gompertz-like sigmoid generated by Eq.(63): (a) The sigmoid ${}^{G}Y_1(\tau)$. (b) The derivative and the sigmoid for $\tau \geq 0$.

Sigmoid with $F_1 = Exp(\tau)$ **and** $F_2 = Erf(\tau)$. In this case the sigmoid construction is

$$ {}^{G}Y_2 = A_2 Exp\left[-b_2 Erf(-\tau)\right] = A_2 e^{-b_2 Erc(-\tau)} = A_2 e^{b_2 Erc(\tau)} \tag{65} $$

and

$$ \frac{d^{G}Y_2}{d\tau} = 2\frac{e^{-x^2}}{\sqrt{\pi}} e^{erf(x)} = 2\frac{e^{erf(x)-x^2}}{\sqrt{\pi}} \tag{66} $$

with asymmetric profile and derivative (see Figure 20) with $A_2 = b_2 = 1$). Further, ${}^{G}Y_2(0) = 1$, as well as ${}^{G}Y_2(-\infty) \to 0.36788$, ${}^{G}Y_2(+\infty) \to 2.7183$. The bell-shaped derivative curve is asymmetric and shifted to the right. Changing the coefficients A,b, etc., the sigmoid can be manipulated to reach desired properties, and normalize, too (issues not discussed further here).

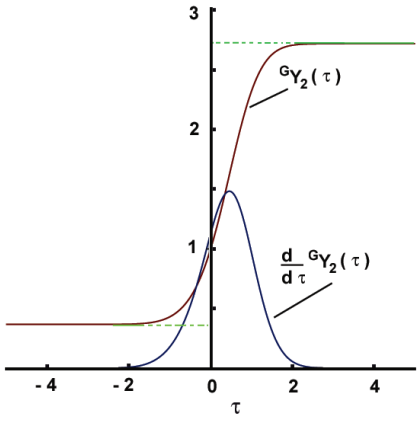

(a)

Figure 20. Gompertz-like sigmoid and its derivative generated by Eq.(65) and Eq. (66).

Sigmoid with $F_1 = Erfc(\tau)$ ***and*** $F_2 = Erfc(\tau)$. In this case, completely involving the complimentary error function the sigmoid formulation is

$$ {}^{G}Y_3 = A_3 Erfc\left[-b_3 Erfc(-\tau)\right] \tag{67} $$

and

$$ \frac{d^{G}Y_3}{d\tau} = \frac{4}{\pi} e^{-x^2} e^{-erfc(-x)^2} = \frac{4}{\pi} e^{-\left[x^2 + erfc(-x)^2\right]} \tag{68} $$

both of them asymmetric (see Figure 21-panel (a))) with asymptotes: ${}^{G}Y_3(-\infty) \to 1$, and ${}^{G}Y_3(+\infty) \to 1.9553$; also ${}^{G}Y_3(0) = 1.8427$.

It can be normalized by a rescaling (see the same procedure with Eq. (59) above)

$$ {}^{G}Y_{3(rescaled)} = \left(\frac{{}^{G}Y_3/2 - B}{1 - B} \right) = \left(\frac{{}^{G}Y_3/2 - {}^{1}/_{2}}{1/2} \right), \quad B = 1/2 \tag{69} $$

Now, it is ${}^{G}Y_{3(rescaled)}(-\infty) \to 0$ and ${}^{G}Y_{3(rescaled)}(+\infty) \to 1$, but at $\tau = 0$ we have ${}^{G}Y_{3(rescaled)}(0) \approx 0.8427$ (see Figure 21-panel (b)).) Changing the coefficients A_3 and b_3, as well as the rescaling parameter B we may create sigmoids with different asymmetries.

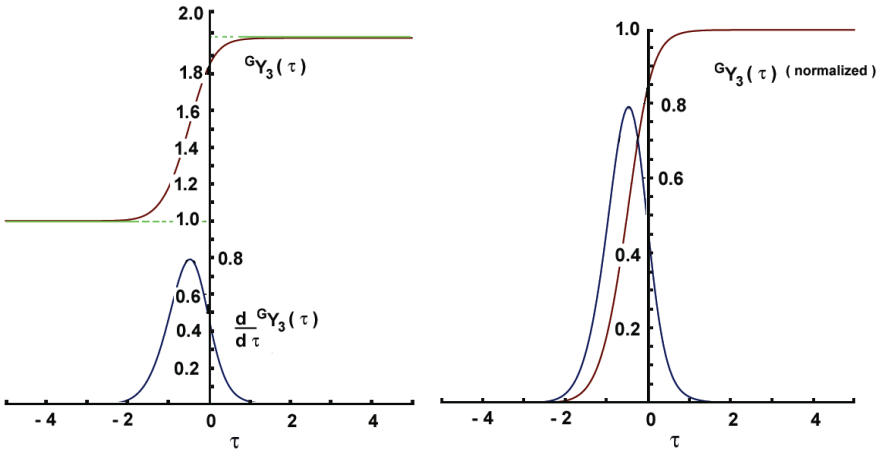

(a) (b)

Figure 21. Gompertz-like sigmoid and its derivative generated by Eq.(67) and Eq. (68): (a) Non-Normalized, (b) Normalized

Computation by Mathematica. All these three sigmoids (non-normalized) just analyzed above are shown Figure 22

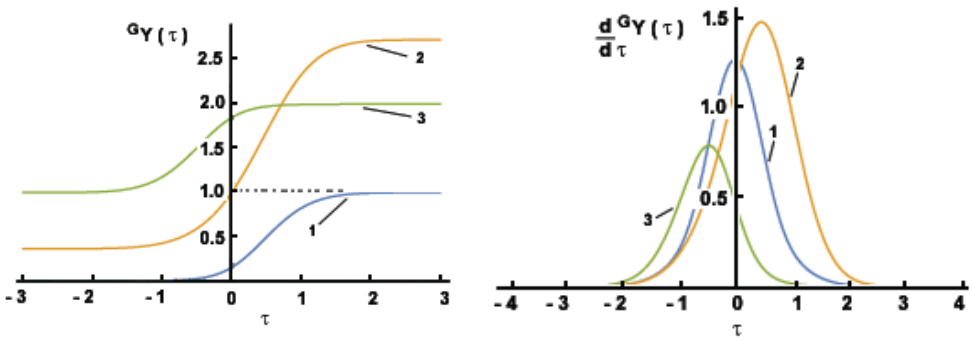

(a) (b)

Figure 22. Gompertz-like sigmoids, (non-normalized) and their derivatives simulated by Mathematica. (a) Sigmoids: 1-Eq.(63), 2- Eq.(65) , 3- Eq.(67). (b) Derivatives:1-Eq.(64), 2- Eq.(66), 3-Eq.(68)

3.3.6. Gompertz-like sigmoids with $E_\alpha(-\tau^\alpha)$ and $E_\beta(-\tau^\beta)$:The concept

After the specific case of Gompertz-like sigmoid considered in the preceding section, let us now consider the general case where both functions are Mittag-Leffler functions of one parameter.

Hence, the construction suggested is

$$ {}^{G}Y_{\alpha,\beta} = AF_1\left[F_2\left(x\right)\right] \Rightarrow AE_\alpha\left[-E_\beta\left(-x^\beta\right)^{-\alpha}\right], \quad \alpha \neq \beta, \quad 0 < \alpha \leq 1, \quad 0 < \beta \leq 1 \tag{70} $$

or more explicitly, assuming for the sake of simplicity $A = 1$, we may write

$$ {}^{G}Y_{\alpha,\beta} = \sum_{k=0}^{N} \frac{(-1)^k \left[\sum\limits_{k}^{N} \frac{(-1)^k \tau^{-\alpha k}}{\Gamma(\alpha k+1)}\right]^{-\beta k}}{\Gamma\left(\beta k+1\right)}, \quad \alpha \neq \beta, \quad 0 < \alpha \leq 1, \quad 0 < \beta \leq 1 \tag{71} $$

For $\alpha = \beta = 1$ (71) reduces to the classical Gompertz construction.

Following the formulation (71), we have two general cases: a case with $\alpha < \beta$ and a case with $\alpha > \beta$, both shown in Figure 23-panels (b) and (c). As might be expected, the plots do not cross the ordinate either at points ${}^{G}Y(0, 1/2)$ or ${}^{G}Y(0, 0)$, a behavior completely corresponding to the entire class of Gompertz-like formulations considered here. Both cases in panels (b) and (c) seem similar but have different cross points with the ordinate at $\tau = 0$. Moreover, this formulation has no branches for $\tau < 0$. In general, it is less flexible than the formulations discussed in the preceding section.

The formulations and the plots presented in Figure 23 are only the first steps in such general definitions that need further analysis and detailed studies, not in the scope of this work. In general, correct simulations by Maple need at least $N = 150$, which is not a problem in terms of computing time required.

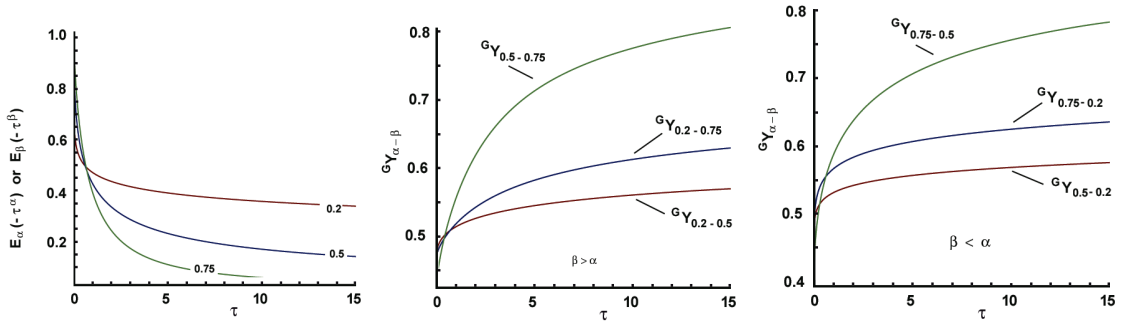

(a) **(b)** **(c)**

Figure 23. Gompertz-like sigmoids with $E_\alpha\left(-\tau^\alpha\right)$ and $E_\beta\left(-\tau^\beta\right)$ for $\tau \geq 0$: (a) The used Mittag-Leffler Functions, (b) ${}^{G}Y_{\alpha,\beta}$ for $\beta > \alpha$, (c) ${}^{G}Y_{\alpha,\beta}$ for $\beta < \alpha$.

Two extremes. Two extremes are interesting to consider, namely:

- For $0 < \alpha < 1$ and $\beta = 1$ we have

$$ {}^{G}Y_{\alpha,1} = E_\alpha\left[-exp(-\tau)\right] = \sum_{k=0}^{N} \frac{(-1)^k \left[-exp(-\tau)\right]^{\alpha k}}{\Gamma(\alpha k+1)} \tag{72} $$

  In a particular case, for instance, $E_{1/2,1}\left[-exp(-\tau)\right] = e^{[e^{-\tau}]^2 erfc[e^{-\tau}]}$(see Eq.(47) in Section 3.3.1).

- For $alpha = 1$ and $< \beta < 1$ we have

$$ {}^{G}Y_{1,\beta} = exp[-E_\beta(-\tau^\beta)] = exp\left[-\sum_{k=0}^{N} \frac{(-1)^k \tau^{\beta k}}{\Gamma(\beta k+1)}\right] \tag{73} $$

  For $\tau = 0$ we have ${}^{G}Y_{1,\beta}(0) \approx 0.36779$, while ${}^{G}Y_{1,\beta}(\infty) \to 1$. Moreover, this extreme case generates sigmoids, which are easily tractable in contrast to the other extreme with $\beta = 1$.

The plots of these two extremes are shown in Figure 24.

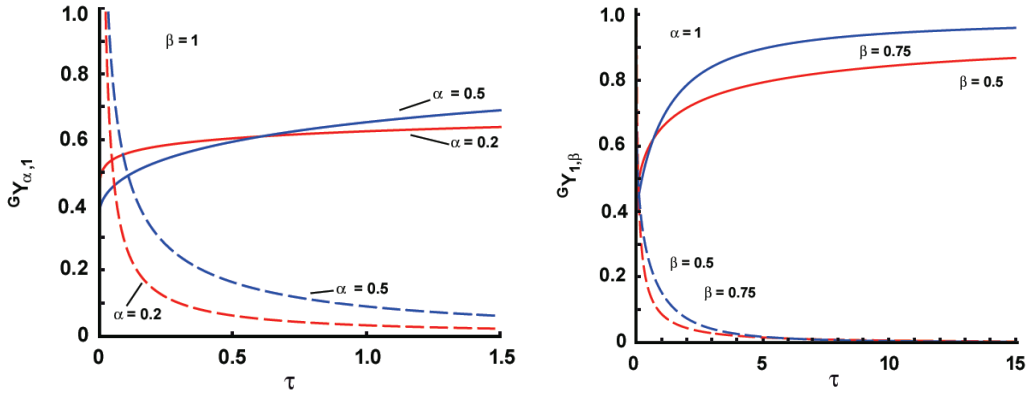

Figure 24. Gompertz-like sigmoids with $E_\alpha\left(-\tau^\alpha\right)$ and $E_\beta\left(-\tau^\beta\right)$ for $\tau \geq 0$ (solid lines) and their derivatives (dashed lines): (a) Case with $\beta = 1$ and $0 < \alpha < 1$. (b) Case with $\alpha = 1$ and $0 < \beta < 1$.

4. Sigmoids based on Mittag-Leffler functions of two parameters

In this section we consider two branches pertinent to $E_{\alpha,\beta}(-\tau^\alpha)$ and $E_{\alpha,\beta}(\tau^\alpha)$ providing different sigmoid functions.

4.1. Sigmoids based on $E_{\alpha,\beta}(-\tau^\alpha)$

Let us now consider a case where the exponential in (2) is replaced by the Mittag-Leffler function of two parameters $E_{\alpha,\beta}(-\tau^\alpha)$ as its generalization, namely

$$Y_{ML(\alpha,\beta)} = \frac{1}{1 + C_2 E_{\alpha,\beta}\left(-rt^\alpha\right)} = \frac{1}{1 + C_2 E_{\alpha,\beta}\left(-\tau^\alpha\right)} \tag{74}$$

From $t = 0 \Rightarrow \tau = 0$ it follows that $C_2 = 1$ because for $t = 0$ we have $E_{\alpha,\beta}(-\tau^\alpha)_{\tau=0} = 1$, and $Y_{ML2}\left(\tau = 0\right) = 1/2$. Now, we are interested in what rate equation could lead to this function as a solution. First, let us rearrange Eq.(74) as

$$\frac{1}{Y_{ML(\alpha,\beta)}} = 1 + E_{\alpha,\beta}\left(-\tau^\alpha\right) \rightarrow \frac{1}{Y_{ML2}} - 1 = E_{\alpha,\beta}\left(-\tau^\alpha\right) \tag{75}$$

Then, denoting $\frac{1}{Y_{ML(\alpha,\beta)}} - 1 = \frac{1 - Y_{ML(\alpha,\beta)}}{Y_{ML(\alpha,\beta)}} = \Theta_{2(\alpha,\beta)}\left(\tau\right)$, we get

$$\Theta_{2(\alpha,\beta)}\left(\tau\right) = E_{\alpha,\beta}\left(-\tau^\alpha\right) \tag{76}$$

Now, we have to stress the attention on the fact that $E_{\alpha,\beta}\left(-\tau^\alpha\right)$ is an extension of $E_\alpha\left(-\tau^\alpha\right)$ but not a solution of a fractional differential equation similar to (24), and therefore we have to look for some special cases, as those summarized in Appendix B (see Section 9.2.3).

4.2. Cases with $E_{\alpha,\beta}(-\tau^\alpha)$

Case with $\alpha = \beta = 1$. In this simplest case $E_{1,1}\left(-\tau\right) = e^{-\tau}$, and we reach the classic Verhulst model, that is

$$\Theta_2(\tau)_{(\alpha=\beta=1)} = e^{-\tau} \Rightarrow \frac{1}{Y_{ML(\alpha=\beta=1)}} - 1 = e^{-\tau} \Rightarrow Y_{ML(\alpha=\beta=1)} = \frac{1}{1 + e^{-\tau}} \tag{77}$$

Case with $\alpha = 1$, $\beta = 2$. In such a case, we have (see Eq.(160) in Appendix B (Section 9.2.3))

$$E_{1,2}\left(-\tau\right) = \frac{e^{-\tau} - 1}{-\tau} = \frac{1 - e^{-\tau}}{\tau} \tag{78}$$

Further, we have $\lim_{\tau \to 0^+} E_{1,2}\left(-\tau\right) = 1$, and it follows that $E_{1,2}\left(-\tau\right)$ is bounded at the origin and decaying faster with an increase in τ (see Figure 25-panel (a)); also, $E_{\alpha,\beta}\left(-\tau\right)$ for $0 \leq \alpha \leq 1$, and $\beta > \alpha$ is completely monotone [32].

Now, let us consider the construction

$$Y_{ML(\alpha=1,\beta=2)} = \frac{1}{1+C_3 E_{1,2}\left(-\tau\right)} = \frac{1}{1+C_3 E_{1,2}\left(-\tau\right)} \tag{79}$$

with $\lim_{\tau\to 0^+} E_{1,2}\left(-\tau\right)=1$ it follows that $Y_{ML(\alpha=1,\beta=2)}\left(\tau=0\right)=1/2$. Moreover, as $\tau\to\infty$ we have $Y_{ML(\alpha=1,\beta=2)_{(t\to\infty)}}\to 1$.

Hence, $Y_{ML(\alpha=1,\beta=2)}$ exhibits all general properties of a logistic function, which is non-symmetric with respect to $\tau=0$ (see Figure 25-panel (b)), and, therefore, we may write

$$Y_{ML(\alpha=1,\beta=2)} = \frac{1}{1+E_{1,2}\left(-\tau\right)} = \frac{\tau}{1+\tau-e^{-\tau}} \tag{80}$$

where $Y_{ML(\alpha=1,\beta=2)}\left(-\infty\right)=0$, $Y_{ML(\alpha=1,\beta=2)}\left(0\right)=1/2$ and $Y_{ML(\alpha=1,\beta=2)}\left(\infty\right)=1$.

The following transform

$$\frac{1}{Y_{ML(\alpha=1,\beta=2)}} = 1+E_{1,2}\left(-\tau\right) \Rightarrow \frac{1-Y_{ML(\alpha=1,\beta=2)}}{Y_{ML(\alpha=1,\beta=2)}} = \frac{1-e^{-\tau}}{\tau} \tag{81}$$

but, (81) does not lead to any idea about a governing differential equation, so (79) can be considered as an empirically constructed logistic function.

However, if we consider $Y_{ML(\alpha=1,\beta=2)}$ as a cumulative distribution, then its derivative with respect to τ yields a bell-shaped asymmetric curve, like a left-shifted normal distribution (see Figure 25-panel (c)).

$$\frac{dY_{ML(\alpha=1,\beta=2)}}{d\tau} = \frac{1}{e^{\tau}}\frac{1-(1+\tau)}{\left((1+\tau)-e^{-\tau}\right)^2} \tag{82}$$

and its series approximation is (by Maple)

$$\frac{dY_{ML(\alpha=1,\beta=2)}}{d\tau} \approx \frac{1}{8}-\frac{\tau}{48}-\frac{\tau^2}{128}+\frac{17}{5760}+\frac{\tau^4}{18432}-\frac{251}{1290240}\tau^5+O(\tau^6) \tag{83}$$

Respectively, we may approximate by a series $Y_{ML(\alpha=1,\beta=2)}\left(\tau\right)$ (by Maple) as

$$Y_{ML(\alpha=1,\beta=2)} \approx \frac{1}{2}+\frac{\tau}{8}-\frac{\tau^2}{96}-\frac{\tau^3}{384}+\frac{17}{23040}\tau^4+\frac{\tau^5}{92160}-\frac{251}{7741440}\tau^6+O(\tau^7) \tag{84}$$

and these approximations may facilitate the calculations.

4.3. Asymptotics with $\alpha=1$, $\beta=2$

From Eq. (170) (see Appendix B) we have

$$E_{\alpha,\beta}\left(-\tau^{\alpha}\right) \approx \exp\left[-\frac{\tau^{\alpha}}{\Gamma\left(\alpha+\beta\right)}\right], \quad \tau\to 0 \tag{85}$$

Then, for $\tau\to 0$ the logistic function (74), with $C_2=1$, can be approximated as

$$Y_{ML(\alpha,\beta)_{(t\to 0)}} \approx \frac{1}{1+e^{-\frac{\tau^{\alpha}}{\Gamma(\alpha+\beta)}}} \tag{86}$$

and it can be considered as a solution to

$$\frac{dY_{ML(\alpha,\beta)}}{d\tau} = -\frac{1}{\Gamma\left(\alpha+\beta\right)}Y_{ML(\alpha,\beta)}\left(1-Y_{ML(\alpha,\beta)}\right) \tag{87}$$

or in terms of the observation time as

$$\frac{dY_{ML(\alpha,\beta)}}{dt} = -\frac{r}{\Gamma\left(\alpha+\beta\right)}Y_{ML(\alpha,\beta)}\left(1-Y_{ML(\alpha,\beta)}\right) \tag{88}$$

Further, with

$$E_{\alpha,\beta}\left(-\tau^{\alpha}\right) \approx \sum_{k=1}^{\infty}\left(-1\right)^{k-1}\frac{\tau^{-\alpha k}}{\Gamma\left(\beta-\alpha k\right)}, \quad \tau\to\infty \tag{89}$$

we may extend the series as

$$E_{\alpha,\beta}\left(-\tau^{\alpha}\right)\approx\frac{\tau}{\Gamma\left(\beta-\alpha\right)}+\frac{\tau^{-2\alpha}}{\Gamma\left(\beta-2\alpha\right)}+\sum_{k=3}^{\infty}\left(-1\right)^{k-1}\frac{\tau^{-\alpha k}}{\Gamma\left(\beta-\alpha k\right)} \tag{90}$$

and it is hard to construct a well-defined logistic function. This situation became clearer in the specific case with $\alpha=1$ and $\beta=2$ (see further Eq.(93) and the emerging problems in calculations).

Case with $\alpha=1$, $\beta=2$ ***and asymptotes at the origin***. In this case we have $E_{1,2}\approx\exp\left[-\frac{t}{\Gamma(3)}\right]$ and the approximation of $Y_{ML(\alpha=1,\beta=2)}\left(t\rightarrow0^{+}\right)$ is

$$Y_{ML(\alpha=1,\beta=2)}\left(\tau\rightarrow0^{+}\right)=\frac{1}{1+e^{-\frac{\tau}{\Gamma(3)}}}=\frac{1}{1+e^{-\frac{\tau}{2}}} \tag{91}$$

with a rate constant $r=1/\Gamma\left(3\right)\approx1/2$, and it is a solution to the Verhulst model

$$\frac{dY_{ML(\alpha=1,\beta=2)}}{d\tau}=\frac{1}{2}Y_{ML(\alpha=1,\beta=2)}\left(1-Y_{ML(\alpha=1,\beta=2)}\right) \tag{92}$$

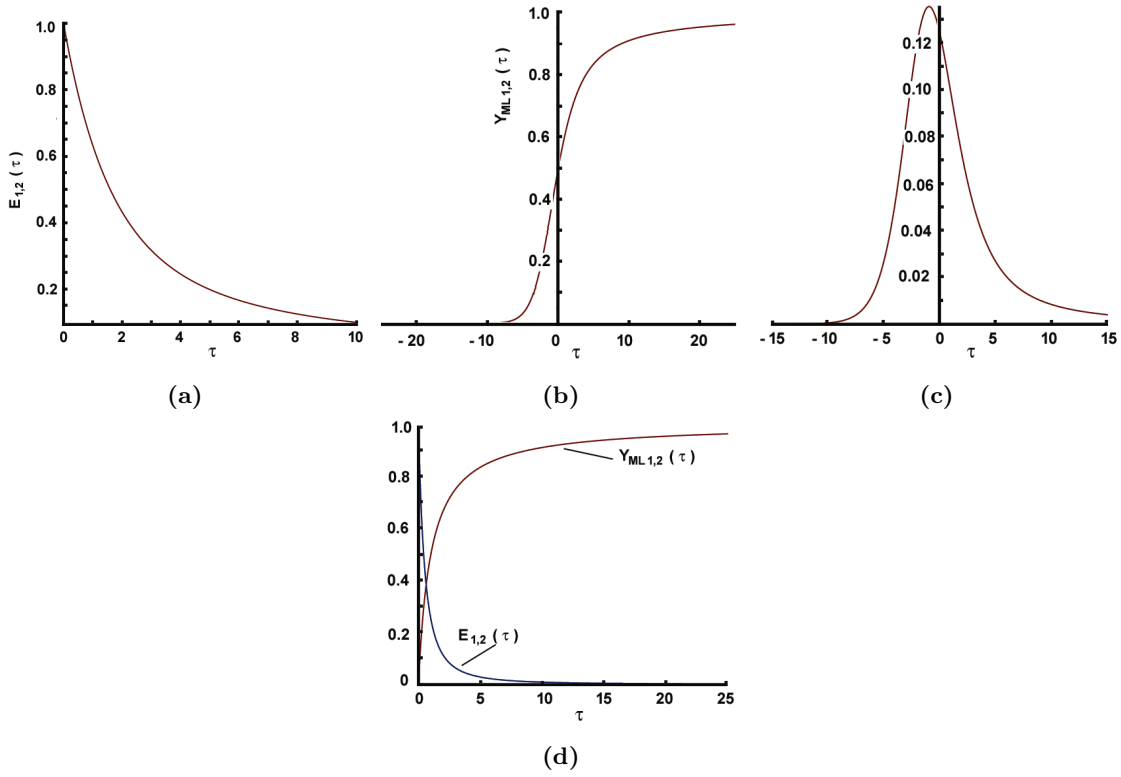

Figure 25. Logistic-type functions based on $E_{1,2}(\tau)$: (a) The bounded function $E_{1,2}$; (b) The resultant logistic curve; (c) The derivative with respect to τ considered as a PDF of the logistic law ; (d) The function $E_{1,2}(\tau)$ and $Y_{ML(\alpha=1,\beta=2)}$ at large values of τ. Computations done by Maple.

Case with $\alpha=1$, $\beta=2$ ***and asymptotes at infinity***. At infinity, with a first-order approximation we have

$$E_{1,2}\approx\sum_{k=1}^{\infty}\left(-1\right)^{k-1}\frac{\tau^{-k}}{\Gamma\left(2-k\right)}\approx\frac{\tau^{-1}}{\Gamma\left(1\right)} \tag{93}$$

Note: The terms for $k\geq2$ are uncomputable because the arguments of the gamma function become negative.

Hence, with approximation (93) we have

$$Y_{ML(\alpha=1,\beta=2)}\left(\tau\to\infty\right)=\frac{1}{1+\frac{1}{\tau}},\quad \frac{dY_{ML(\alpha=1,\beta=2)}}{d\tau}\left(\tau\to\infty\right)=\frac{1}{\left(1+\tau\right)^{2}} \tag{94}$$

with an almost flat profile of $Y_{ML(\alpha=1,\beta=2)}\left(\tau\to\infty\right)$ and rapidly decreasing $\frac{dY_{ML(\alpha=1,\beta=2)}}{d\tau}\left(\tau\to\infty\right)$ as it is illustrated in Figure 25-panel (d).

4.4. Sigmoids based on $E_{\alpha,\beta}(\tau^{\alpha})$

Here we consider the special case where $E_{\alpha,\beta}(\tau)=E_{2,2}(\tau)$ since it easy can be calculated applying computer algebra codes.

Let us now construct a sigmoid based on $E_{\alpha,\beta}\left(\tau\right)$, precisely the specific case when $\alpha=\beta=2$, allowing $E_{2,2}\left(\tau^{\alpha}\right)$ to be expressed through the hyperbolic sine

$$E_{2,2}\left(\tau\right)=\sum_{k=0}^{\infty}\frac{\tau^{2k}}{\Gamma\left(2k+2\right)}=\frac{\sinh\sqrt{\tau}}{\sqrt{\tau}},\quad \tau>0 \tag{95}$$

where the hyperbolic *sinh(x)* can be expressed explicitly as a Taylor series at zero

$$sinh(x)=x+\frac{x^{3}}{3!}+\frac{x^{5}}{5!}+\frac{x^{73}}{7!}+\ldots=\sum_{k=0}^{\infty}\frac{x^{2k+1}}{(2k+1)!}=\sum_{k=0}^{\infty}\frac{x^{2k+1}}{\Gamma\left(2k\right)} \tag{96}$$

The series is convergent for every complex x, as well it is odd, then only odd exponents appear. $E_{2,2}\left(\tau^{\alpha}\right)$ is a rapidly increasing function (see Figure 26-panel (a)), and the application of the sigmoidal transformation yields

$$Y_{2,2}\left(\tau\right)=\frac{E_{2,2}\left(\tau\right)}{1+E_{2,2}\left(\tau\right)}=\frac{1}{1+\frac{1}{E_{2,2}(\tau)}}=\frac{1}{1+\frac{\sqrt{\tau}}{\sinh\left(\sqrt{\tau}\right)}} \tag{97}$$

The behavior of $E_{2,2}\left(\tau\right)$ for $\tau<0$ in Fugure 26-panels (a) and (b)),can be attributed to the hidden computer code of Maple and the fact that $\sqrt{-\tau}$ is a complex. For more comments see Remark 9 below.

Since $\frac{\sinh\sqrt{\tau}}{\sqrt{\tau}}$ for $\tau\to0^{+}$ approaches 1, then $Y_{2,2}\left(0\right)=1/2$ as the classical logistic sigmoid. Moreover, we have $Y_{2,2}\left(+\infty\right)=1$ .For $\tau<0$ we have an oscillating $Y_{2,2}\left(-\tau\right)$ as it is shown in Figure 26-panel (b) and could be attributed to unpredictable behavior of the Maple code.

The reduction

$$\bar{Y}_{2,2}\left(\tau\right)=\frac{Y_{2,2}\left(\tau\right)-B}{1-B},\quad B=\frac{1}{2} \tag{98}$$

results in $\bar{Y}_{2,2}\left(0\right)=0$ with an asymptote $\bar{Y}_{2,2}\left(+\infty\right)=1$ that converges with that of $Y_{2,2}\left(+\infty\right)=1$. Hence, the pragmatic approach is that $Y_{2,2}\left(\tau\right)$ and $\bar{Y}_{2,2}\left(\tau\right)$ are useful for applications and data fitting.

The computations done by Maple directly used the hyperbolic sine function $\sinh\left(x\right)$ but the question about the calculation method remains. The question about the number of terms in a truncated series $E_{2,2}\left(\tau;N\right)$ invoked experiments shown in Figure 26-panel (c) . The simulation through truncated series yields symmetrical sigmoids with $Y_{2,2}\left(0\right)=1/2$ that can be easily reduced by applying (98). The simulation tests reveal that even 5 terms in the truncated series are enough and for $N>5$ all plots match (see Figure 26-panel (c)).

It is worth noting that the sigmoids generated directly through $E_{2,2}\left(\tau\right)=\frac{\sinh\sqrt{\tau}}{\sqrt{\tau}}$ need larger values of τ, $\tau>0$ to attain the asymptote 1, while for those simulated by truncated series, large values τ are needed, as demonstrated in Figure 26-panel (d)).

Remark 9 (On the asymmetric and symmetric sigmoids generated by $E_{2,2}\left(\tau\right)$)**.** *At this moment, it is important to recall that the symmetric sigmoids generated by truncated series expansions illustrate the fundamental property ($sinh(-x)=-sinh(x)$). Consequently, we have ($\frac{sinh(-x)}{-x}=-\frac{sinh(x)}{x}$). Unfortunately, when applying ($sinh(x)$) to a negative argument in Maple, the computations failed and produced plots shown in Figure 26 (panel (b)). This issue can be*

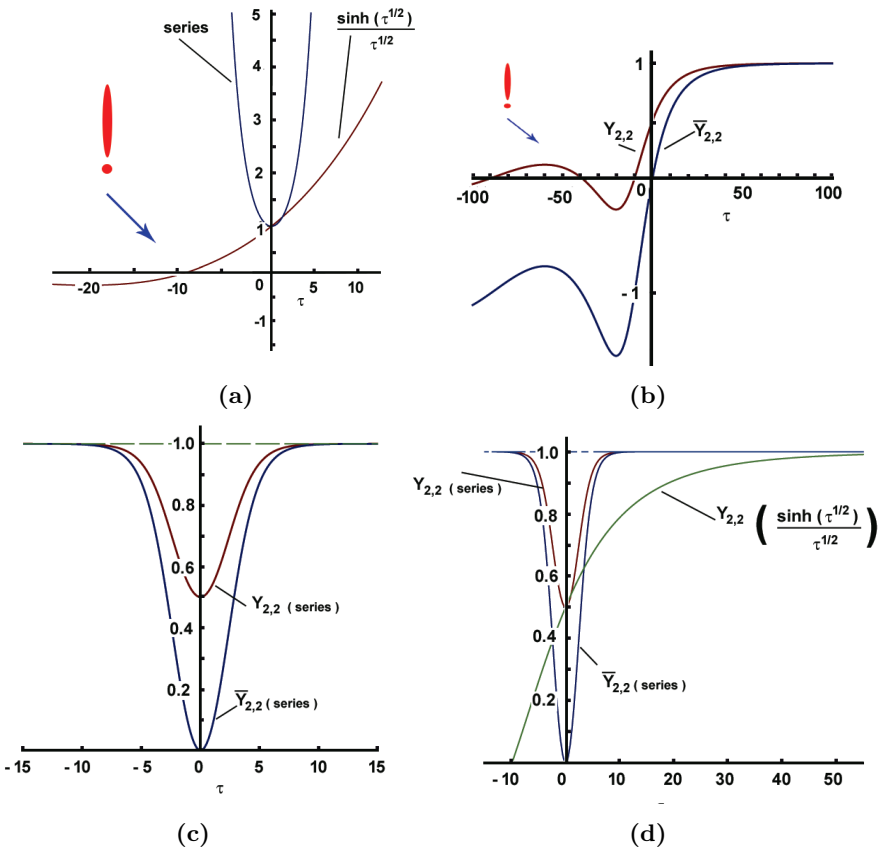

Figure 26. Sigmoids based on $E_{2,2}(\tau)$: (a) The function $E_{2,2}(\tau)$ generated by Maple (using the $sinh(x)$ commend and a truncated series, (b) Sigmoids generated by using $F(\tau) = \frac{\sinh\sqrt{\tau}}{\sqrt{\tau}}$, (c) Sigmoids generated by using truncated series, (d) Comparative plots of the sigmoids generated by $F(\tau) = \frac{\sinh\sqrt{\tau}}{\sqrt{\tau}}$ and truncated series expansions. Computations done by Maple.Note: The marks in the left sectors of panels (a) and (b) stress the attention on what happens if the code is incorrectly.

attributed to the fact that $(\sqrt{-\tau})$ *is complex. Fortunately, this problem does not arise when using the series expansion in equation (95), as all exponents in this expansion are even (i.e., (2k)). Therefore, it does not matter whether calculations are performed with* $(-\tau)$ *or* $(+\tau)$*; in both cases, we obtain symmetrical plots.*

5. Another examples of extended logistic laws

The use of the Mittag-Leffler function in place of the standard exponential function demonstrates that the general framework of the logistic law can be extended to new applications, and the corresponding governing equations can be recovered.

Before proceeding, we aim to establish general conditions that should be applied to functions that fall within the broader category of S-shaped functions, which includes logistic-like functions as a subset. The general definitions will be formulated as follows:

- Logistic-like functions where $Y_{Log}(0) = 1/2$ and $Y_{Log}(\infty) = 1$.
- S-shaped functions where $Y_{Log}(0) = 0$ and $Y_{Log}(\infty) = 1$.

Based on these general definitions, we focus on the properties and conditions that the functions should satisfy, replacing the exponential in the logistic law formulation.

5.1. Requirements and conditions imposed on the candidate functions

Consider the general expressions

$$Y(\tau) = \frac{1}{1+F(\tau)} \tag{99}$$

$$^{A}Y(\tau) = 1 - \frac{1}{1+F(\tau)} = 1 + \frac{1}{F(\tau)} \tag{100}$$

and the question arising is about the property of $F(t)$ allowing it to generate logistic-like laws, or at least S-shaped functions with general conditions $Y(\infty) \to 1$ and $^{A}Y(\infty) \to 0$.

We consider two general situations:

- Cases when the function $F(\tau)$ is bounded at the origin, as in the situation with classical logistic law, and
- Cases when the function $F(\tau)$ is unbounded at the origin

5.1.1. Cases with functions bounded at the origin

Let the function $Y_{log}(\tau)$ satisfies the conditions (as the classical logistic law) :

$$Y(0) = \frac{1}{2}, \quad Y(\infty) = 1 \tag{101}$$

Therefore, $F(\tau)$ should be bounded at $\tau = 0$ (i.e., $F(0) = 1$) and vanish at $\tau = \infty$ (at least at large values of t).

We observed that the Mittag-Leffler function is a suitable candidate, and a natural question arises: are there other functions that may serve a similar role? Obviously, the exponential function $e^{-\tau}$ in the original logistic model is the fastest one (decays to zero in the fastest way compared to the Mittag-Leffler function, which is slower).

The form expressed by (100) can be considered because of the application of the so-called sigmoidal transformation.

$$Y_{Log} = \frac{x^{\alpha}}{1+x^{\alpha}} = \frac{1}{1+x^{-\alpha}} \tag{102}$$

with $\lim_{t\to 0^{+}} Y_{Log} = 1$, and $\lim_{t\to\infty} Y_{Log} = 0$.

A simple change in variables $x = e^{-k\tau}$ yields the well-known logistic law (the solution of the Verhulst model)

$$Y_{Log} = \frac{e^{k\tau}}{1+e^{k\tau}} = \frac{1}{1+e^{-k\tau}} \tag{103}$$

Thus, we may generalize (100) as

$$Y_{Log} = \frac{z}{1+z} = \frac{1}{1+z^{-1}}, \quad z^{-1} = f(\tau) \Rightarrow y = \frac{f(\tau)}{1+f(\tau)} = \frac{1}{1+f(\tau)^{-1}} \quad F(\tau) = \frac{1}{f(\tau)} \tag{104}$$

with $z(0) = 1$ and $z(\infty) \longrightarrow 0$, irrespective of its argument, time, or a spatial coordinate.

Remark 10 (The simple sigmoidal transformation:some clarifications)**.** *To ensure accuracy in defining the simple sigmoidal transformation (103), we will reference another definition known as the simple algebraic sigmoidal transformation conceived in [41] (see also [42,43]) and defined as*

$$Y_{\alpha} = \frac{x^{\alpha}}{x^{\alpha}+(1-x)^{\alpha}}, \quad y_{\alpha}(x) + y_{\alpha}(1-x) = 1, \quad 0 \le x \le 1 \tag{105}$$

where $Y_{\alpha} \in C^{1}[0,1] \cap C^{\infty}(0,1)$ *and* $Y_{\alpha}(0) = 0$*, and* Y_{α} *is strictly increasing on* $[0,1]$*, as well* dY_{α}/dx *strictly increasing on* $[0,1/2]$ *with* $dY_{\alpha}(0)/dx = 0$*.*

5.1.2. Cases with functions unbounded at the origin

The condition (see Eq.(100)) is based on the requirement $Y_{Log}(0) = 1/2$, but the formulation (100) allows another interpretation considering $F(t)$ unbounded at the origin, which allows generating S-shaped curves, i.e.,

$$F(\tau \to 0) \to \infty \Rightarrow Y_{S}(0) = 0, \quad F(\infty) \to 0 \Rightarrow Y_{S}(\infty) = 1 \tag{106}$$

As a result, we find that $Y_S(0) = 0$, indicating that the logistic (S-shaped) function begins at $\tau = 0$ and approaches unity as τ approaches infinity. These scenarios will be discussed further in Section 5.3.

5.2. Examples with $F(\tau)$ bounded at the origin: Logistic-type laws

5.2.1. Lambert functions

Lambert function bounded at the originLet us consider another candidate regarding the Lambert function [44, 46–49] in two versions, bounded (107) and unbounded (108) at the zero, namely

$$L_{WB} = \frac{\alpha\tau}{e^{\alpha\tau} - 1}, \quad \alpha > 0, \quad \tau > 0 \tag{107}$$

with $\lim_{t\to 0^+} L_{WB} \to 1$, $\lim_{t\to\infty} L_{WB} \to 0$. It is non-symmetrical with respect to the ordinate and illustrated in Figure 27-panel (a).

The unbounded at the origin version is

$$L_{WU} = \frac{1}{e^{\alpha\tau} - 1}, \quad \alpha > 0, \quad \tau > 0 \tag{108}$$

with $\lim_{\tau\to 0^+} L_{WU} \to \infty$, $\lim_{t\to\infty} L_{WU} \to 0$. It is symmetrical with respect to the origin (see Figure 27-panel (b)). This function is considered in Section 5.3.1.

In the case of the bounded version (107), which is non-symmetrical with respect to the ordinate (see Figure 27-panel (a)) and satisfying the general condition (101), we have

$$Y_{LB} = \frac{1}{1 + \frac{\alpha\tau}{e^{\alpha\tau}-1}} = \frac{e^{\alpha\tau} - 1}{\alpha\tau + e^{\alpha t} - 1} \tag{109}$$

with $\lim_{t\to 0^+} L_{WU} \to 1/2$, $\lim_{\tau\to\infty} Y_{LB} \to 0$.

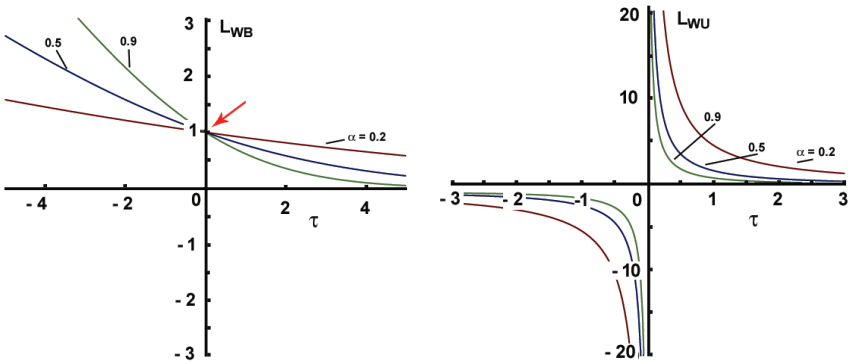

(a) (b)

Figure 27. The Lambert functions at the various values of the parameter α: (a) The bounded function; (b) The unbounded function; Computations done by Maple.

5.3. Examples with $F(\tau)$ unbounded at the origin: S-shaped functions

Now, we address two cases based on the interpretations of the unbounded Lambert function:

- Unbounded Lambert function $F(\tau)$ in its classical singular formulation (110)
- Unbounded Lambert-like $F(\tau)$ function, singular at the origin, and utilizing the Mittag-Leffler function.

5.3.1. $F(\tau)$ as a Lambert function unbounded at the origin

In case of the singular version (108) we get

$$Y_{Lu} = \frac{1}{1 + \frac{1}{e^{\alpha\tau}-1}} = \frac{e^{\alpha t} - 1}{e^{\alpha\tau}} = 1 - e^{-\alpha\tau} \tag{110}$$

which is the simplest version of non-symmetric S-shaped curves with $\lim_{t\to 0^+} Y_{LU} \to 0$ (see Figure 28-panel (b), and $\lim_{t\to\infty} Y_{LU} \to 1$. If we change the variable as $\tau = kt^n$, then we get the Weibull function $W(t) = W_{max}\left(1 - e^{-kt^n}\right)$ with $W_{max} = 1$ [50]; for $n = 1$ and using r instead of k, then $\tau = kt^n = \tau = rt$, as we have used up to this moment. Moreover, in this case, there is no inflection point because $d^2Y_{LU}/d\tau^2 = -\alpha^2 e^{\alpha\tau}$. As illustrations, we show plots of $dY_{LU}/d\tau$ and $d^2Y_{Lu}/d\tau^2$ in Figure 28-panels (c) and (d), respectively.

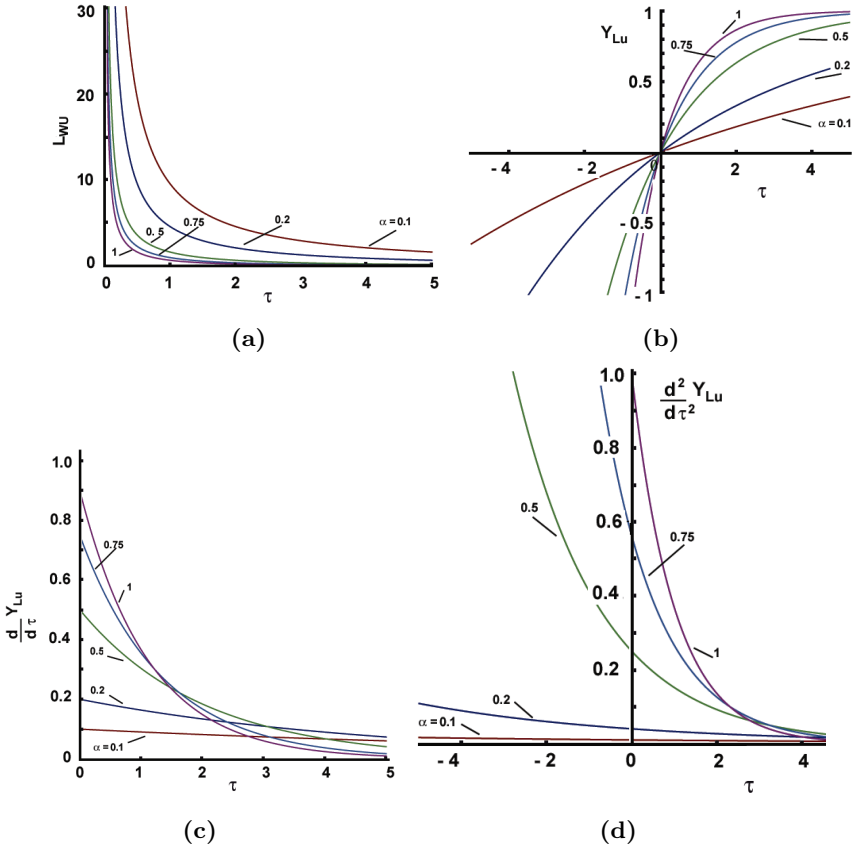

Figure 28. The Lambert function unbounded at the origin at the various values of the parameter α and $\tau \geq 0$, and the resultant distribution: (a) The Function; (b) The resultant distribution (110); (c) The first derivative of (110); (d) The second derivative of (110); Computations done by Maple.

Remark 11 (A consequence of the sigmoidal transformation)**.** *The construction (110) can be considered as a direct consequence of the sigmoidal transformation (103) through the substitution* $x = e^{\alpha\tau} - 1$, *because*

$$Y_{LU} = \frac{(e^{\alpha\tau} - 1)}{1 + (e^{\alpha\tau} - 1)} = \frac{1}{1 + \frac{1}{e^{\alpha\tau} - 1}} \tag{111}$$

The formulation (110) is well-known solution (integral) of the kinetic equation

$$\frac{dY_{Lu}}{d\tau} = -\alpha Y_{Lu} \tag{112}$$

Replacing τ by $\tau = kt^n$, as we already did above, we get

$$\frac{dY_{Lu}}{dt} = -\alpha k t^{n-1} Y_{Lu} \tag{113}$$

Denoting $Y_{Lu} = 1 - Z$ and assuming for now that $\alpha = 1$, we obtain

$$\frac{d\,(1 - Z)}{dt} = -knt^{n-1}\,(1 - Z) \Rightarrow \frac{dZ}{dt} = knt^{n-1}\,(1 - Z) \tag{114}$$

The second form of (114) is the well-known Jonson-Mehl-Avrami-Kolmogorov kinetic equation of phase transformation [51–56]; k is the Avrami constant, while n is the Avrami exponent. It was demonstrated in [57] that assuming the product $\tau = kt^n$ as an independent variable allows for the formulation of a time-nonlocal version of (114), through the Caputo derivative, as $D_\tau^\alpha Z = -kZ$ with a solution in terms of the Mittag-Leffler function of one parameter (see the detailed solution and examples with real data approximations in [57]).

5.3.2. $F(\tau)$ as a Lambert-like function involving Mittag-Leffler functions

Let us consider $F(\tau)$ defined as [49] (illustrated in Figure 29)

$$F\left(\tau\right) = \frac{1}{E_\alpha\left(\tau^\alpha\right) - 1}, \quad 0 < \alpha \leq 1, \quad \tau \geq 0 \tag{115}$$

This definition can be extended as

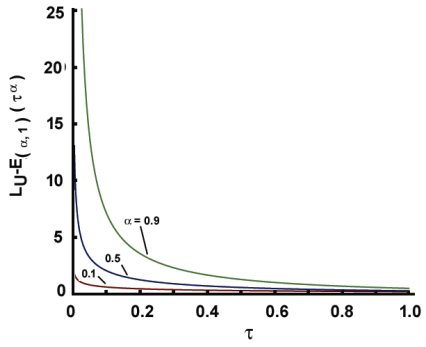

(a)

Figure 29. Unbounded Lambert-like function involving the Mittag-Leffler function of one parameter, $F(\tau) = L_U - E_\alpha)(\tau^\alpha) = (E_\alpha)(\tau^\alpha) - 1)^{-1}$, at the various values of the parameter α. Computations done by Maple.

$$F(\tau) = \frac{1}{\sum_{k=0}^{\infty} \frac{\tau^{\alpha k}}{\Gamma(\alpha k + 1)}} - 1 = \frac{1}{\sum_{k=1}^{\infty} \frac{\tau^{\alpha k}}{\Gamma(\alpha k + 1)}} = \frac{1}{\frac{\tau^\alpha}{\Gamma(\alpha+1} + \frac{\tau^{2\alpha}}{\Gamma(2\alpha+1} + \frac{\tau^{3\alpha}}{\Gamma(3\alpha+1}} \tag{116}$$

The polynomial denominator of the last version of (116) relates this definition to a class of algebraic candidate functions [4–6] but such cases are beyond the scope of this work.

Then, the sigmoid has a construction

$$Y_{LUML1} = \frac{1}{1 + \frac{1}{E_\alpha(\tau^\alpha) - 1}} = 1 - \frac{1}{E_\alpha\left(\tau^\alpha\right)} \tag{117}$$

For instance, for $\alpha = 1$, the term $\frac{1}{E_\alpha(t^\alpha)}$ reduces to $e^{-\alpha\tau}$ and Y_{LUML1} becomes the well-known solution of the Verhulst model. The anti-logistic version of (117) is

$$\frac{1}{1 - Y_{LUML1}} = E_\alpha\left(\tau^\alpha\right) \tag{118}$$

which for $\alpha = 1$ recovers the anti-logistic version of the Verhulst function.

Rearranging (117) as

$$\frac{1}{1 - Y_{LUML1}} = E_\alpha\left(\tau^\alpha\right) \tag{119}$$

We can see that this is the solution to

$$D_t^\alpha \Phi_{ML1} = \Phi_{ML1}, \quad \Phi_{ML1} = \frac{1}{1 - Y_{LUML1}} \tag{120}$$

The computation experiments illustrated in Figure 30 with different numbers of terms in a truncated $E_\alpha\left(\tau^\alpha\right)$ series reveal very stable (smooth) plots even for very low N. This can be

easily understood if we use the latest version of (116) to formulate the logistic law, namely

$$Y_{LUML1} = 1 - \frac{1}{E_\alpha(\tau^\alpha)} = 1 - \frac{1}{1 + \frac{\tau^\alpha}{\Gamma(\alpha+1)} + \frac{\tau^{2\alpha}}{\Gamma(2\alpha+1)} + \frac{\tau^{3\alpha}}{\Gamma(3\alpha+1)} \cdots}, \quad 0 < \alpha \leq 1, \quad t > 0 \tag{121}$$

where $Y_{LUML1}(\tau = 0) = 0$ and $Y_{LUML1}(\tau \to \infty) = 1$.

For example, with $N = 1$ we have $Y_{LUML1}(N = 1) = 1 - \frac{1}{1 + \frac{\tau^\alpha}{\Gamma(\alpha+1)}}$, a simple reciprocal function. Also, for $N = 4$, for instance, we have

$$Y_{LUML1}(N = 4) = 1 - \frac{1}{1 + \frac{\tau^\alpha}{\Gamma(\alpha+1)} + \frac{\tau^{2\alpha}}{\Gamma(2\alpha+1)} + \frac{\tau^{3\alpha}}{\Gamma(3\alpha+1)} + \frac{\tau^{4\alpha}}{\Gamma(4\alpha+1)}}, \quad 0 < \alpha \leq 1, \quad t > 0 \tag{122}$$

Hence, we have a polynomial version of $F(\tau)$ obeying the required condition, yielding S-shaped curves starting from $\tau = 0$ and asymptotically approaching unity. As to the anti-logistic version, we have

$${}^{A}Y_{LUML1} = \frac{1}{1 + \frac{\tau^\alpha}{\Gamma(\alpha+1)} + \frac{\tau^{2\alpha}}{\Gamma(2\alpha+1)} + \frac{\tau^{3\alpha}}{\Gamma(3\alpha+1)} \cdots}, \quad 0 < \alpha \leq 1, \quad t > 0 \tag{123}$$

with ${}^{A}Y_{LUML1}(\tau = 0) = 1$ and ${}^{A}Y_{LUML1}(\tau \to \infty) \to 0$.

As a detectable effect from these computations, we can see that with a low number of terms in the truncated series expansion of $E_\alpha(\tau^\alpha)$, there is a need for large values of τ to reach the saturation level, while for $N = 10$, this asymptotic level can be reached faster; obviously, the increase in the number of terms is an effect of the superposition of exponential terms $\frac{\tau^{\alpha k}}{\Gamma(\alpha k+1)}$, and in each specific case corresponding to a given value of α the number of terms could be determined experimentally.

Remark 12 (The construction (117) as a consequence of the sigmoidal transformation)**.** *The construction (110) can be considered as a direct consequence of the sigmoidal transformation (103) through the substitution $x = E_\alpha(\tau^\alpha) - 1$, because*

$$Y_{LUML1} = \frac{(E_\alpha(\tau^\alpha) - 1)}{1 + (E_\alpha(\tau^\alpha) - 1)} = \frac{1}{1 + \frac{1}{E_\alpha(\tau^\alpha) - 1}} \tag{124}$$

Case with $E_{1/2,1}(-\tau^\alpha)$***:*** Now, consider a case with $E_{\alpha,1}(-\tau^\alpha)$ where (for the properties of $E_{\alpha,1}(-\tau^\alpha)$ see the preceding Section 3.3.1)

$$E_{1/2\,,1}(z) = e^{z^2} erfc(-z) \tag{125}$$

$E_{1/2\,,1}(-\tau^\alpha)$ is bounded at the origin and vanishes for large τ, while the function $F(\tau) = \frac{1}{E_{1/2\,,1}(\tau) - 1}$ is unbounded, thus obeying all properties allowing the logistic-type construction

$$Y_{LUML_{(1/2,1)}} = \frac{1}{\frac{1}{E_{1/2,1}(\tau)} - 1} = \frac{E_{1/2,1}(\tau) - 1}{E_{1/2,1}(\tau)} = 1 - \frac{1}{E_{1/2,1}(\tau)} \tag{126}$$

The plots of $Y_{LUML(1/2,1\,)}\left(-\tau^{1/2}\right)$ and $\frac{dY_{LUML(1/2,1\,)}\left(-\tau^{1/2}\right)}{d\tau}$ are shown in Figure 31-panel (a). The shape is of a logistic type, asymmetric and with $Y_{LUML(1/2,1\,)}(+\infty) = 0.66667$.

If we consider $Y_{LUML(1/2,1\,)}\left(-\tau^{1/2}\right)$, as CDF of distribution, then we have : $Y_{LUML(1/2,1\,)}(-\infty) = 0$, $Y_{LUML(1/2,1\,)}(0) = 1/2$, but $Y_{LUML(1/2,1\,)}(+\infty) = 0.66667$. Hence, for positive τ, the condition $Y_{LUML(1/2,1\,)}(+\infty) = 1$ is not obeyed but this can be corrected if $Y_{LUML(1/2,1\,)}\left(-\tau^{1/2}\right)$ is rescaled by $Y_{LUML(1/2,1\,)}(+\infty)$, as

$$Y_{LUML(1/2,1\,)} = \frac{Y_{LUML(1/2,1\,)}\left(-\tau^{1/2}\right)}{Y_{LUML(1/2,1\,)}(+\infty)} = \frac{Y_{LUML(1/2,1\,)}\left(-\tau^{1/2}\right)}{0.66667} \tag{127}$$

and the results are shown in Figure 31-panel (b).

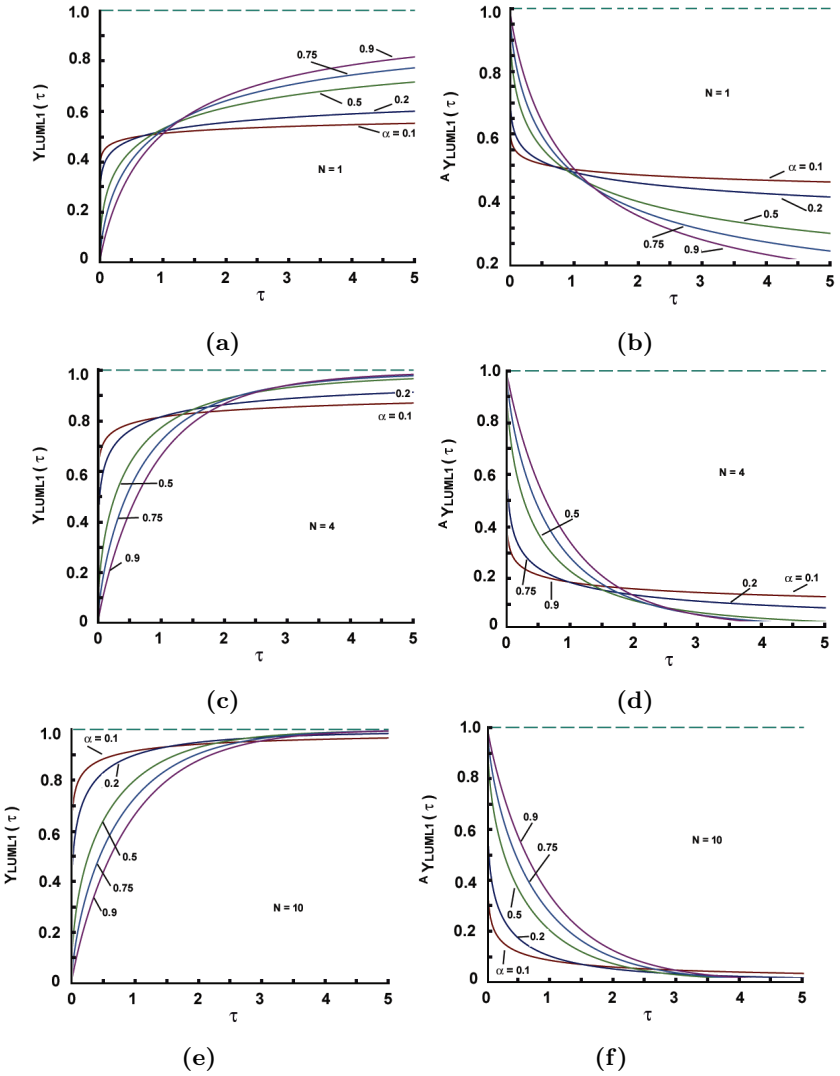

Figure 30. Logistic law with a unbounded Lambert-like function involving the Mittag-Leffler function of one parameter, at the various values of the parameter α and different terms of the truncated Taylor expansion of the Mittag-Leffler function. Left column: Logistic (S-shaped) plots (a),(c), and (e); Right column: Anti-Logistic (Anti S-shaped) plots (b), (d), and (f). Computations done by Maple.

Now, with $\bar{Y}_{LUML(1/2,1\,)}\left(-\tau^{1/2}\right)$ we have a function that satisfies the condition of CFD, that is, $\bar{Y}_{LUML(1/2,1\,)}\left(+\infty\right)=1$. In both cases, with the original and the rescaled CDF, the corresponding PDFs are bell-shaped and left-shifted with respect to the vertical axis.

Case with $E_{2,2}\left(\tau\right)$***:*** After the experiments in Section 4.4 and considering the methods for calculating $E_{2,2}\left(\tau\right)=\sinh\left(\sqrt{\tau}\right)/\sqrt{\tau}$, we proceed to construct a sigmoid using the sigmoidal transformation

$$Y_{LUML-E_{2,2}}\left(\tau\right)=\frac{E_{2,2}\left(\tau\right)-1}{1+\left(E_{2,2}\left(\tau\right)-1\right)}=\frac{1}{1+\frac{1}{E_{2,2}(\tau)-1}},\tau>0 \tag{128}$$

Since $E_{2,2}(0)=1$, it follows that ($\frac{1}{E_{2,2}(\tau)-1}$) is unbounded at the origin. Consequently, we have $\frac{Y_{LUML-E_{2,2}}(\tau\rightarrow0^{+})=0}{}$, indicating the presence of a sigmoid function, specifically, an S-shaped curve that begins at zero and approaches $Y_{LUML-E_{2,2}}(\tau\rightarrow+\infty)=1$. The plots in Figure 32-panel (a) illustrate the symmetric curves generated by the series expansion. Panel (b) focuses on a comparison between computations performed directly in Maple using the command $\frac{\sinh(\sqrt{\tau})}{\sqrt{\tau}}$ and

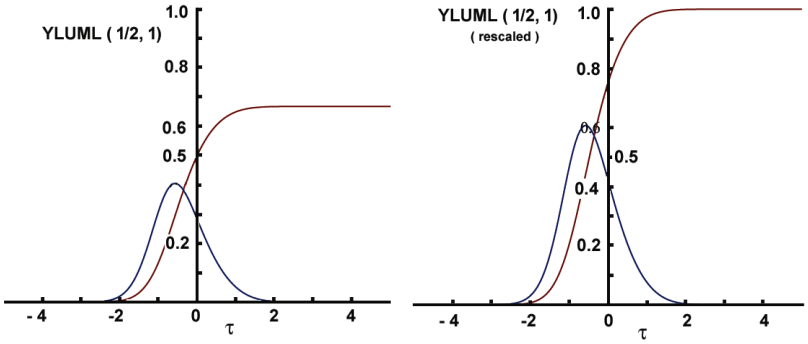

(a) (b)

Figure 31. Unbounded Lambert-like function involving the Mittag-Leffler function $E_{1/2,1}$: (a) $Y_{LUML(1/2,1\,)}$ (red color online) and its derivative (blue color online). (b) Corrected $Y_{LUML(1/2,1\,)}$ and its derivative (the colors are the same as in fig (a). Computations done by Maple.

the truncated series with varying numbers of terms. Panel (c) demonstrates the effect of the number of term in the truncated series that with less 5 terms the plots are distinguishable but beyond 15 there are indistinguishable curves.

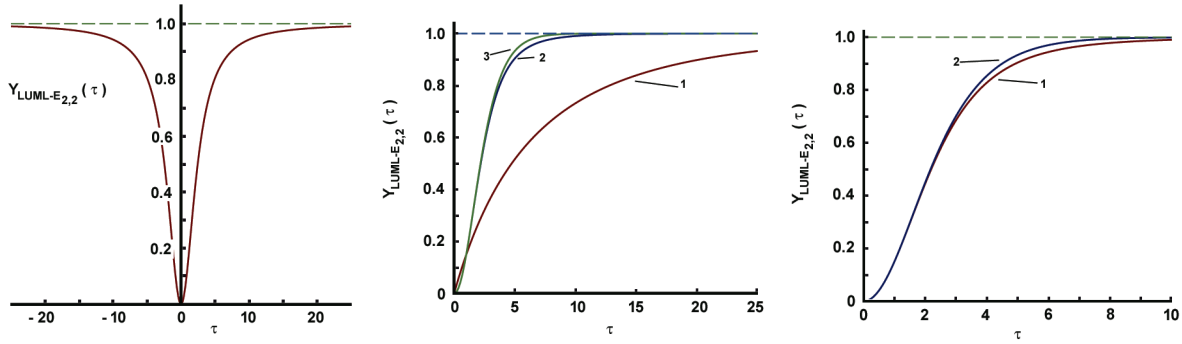

(a) (b) (c)

Figure 32. S-shaped curves generated by $E_{2,2}(\tau)$ and (128). (a) Symmetric sigmoids generated by truncated series expansions with 15 terms. (b) Comparative plots of the sigmoids generated by $\frac{\sinh(\sqrt{\tau})}{\sqrt{\tau}}$ (line 1) and those obtained by truncated series (line 2- 5 terms, and line 3- 15 terms). (c) Effect of the number of terms in the truncated series (as experiment: line $1-2$ terms, line $2-5$ terms). Computations done by Maple.

6. Logistic and sigmoid functions with rates controlled by a non-integer parameter

6.1. The main idea

Here, we try to introduce an idea that will allow us to use some elements of the non-local modeling, precisely from fractional calculus [58, 59] (see details and applications is [60–64]) . Precisely, in the logistic model (1), the rate constant r is defined in the range $r \in (0, \infty)$ but can be mapped as $r = \frac{\alpha}{1-\alpha}$, with $\alpha \in (0, 1)$. Thus, we can write

$$r = \frac{\alpha}{1-\alpha} \Rightarrow \alpha = \frac{r}{1+r} \tag{129}$$

This transformation allows for formulating two types of logistic laws in the sense of those already formulated in the preceding sections: A logistic law with an exponential of a Caputo-Fabrizio

type (Section 6.2) and a Mittag-Leffler function in the Atangana-Baleanu formulation (Section 6.3).

6.2. A logistic law with an exponent of Caputo-Fabrizio type

Following the general suggestion (129) the classical logistic law can be expressed as

$$y_\alpha = \frac{1}{1 + e^{-\frac{\alpha}{1-\alpha}(z - z_0)}} \tag{130}$$

and without difficulties, we can see that the governing equation is

$$\frac{dy_\alpha}{dz} = \frac{\alpha}{1-\alpha} y_\alpha \left(1 - y_\alpha\right) \tag{131}$$

From a model construction perspective, this small modification allows us to demonstrate how we can control the growth of the logistic curve by a non-integer parameter $\alpha \in (0, 1)$. As commented at the beginning, the dimension $r$is in inverse proportion to the dimensions of the argument z. Here, we could face a small confusion since the parameter α is dimensionless. To avoid this, we may present the product rz as

$$rz = \left(rZ_{\max}\right)\left(\frac{z}{Z_{\max}}\right) \tag{132}$$

where $Z_{\max}$ is the characteristic scale such that $z = Z_{\max}$ we have $y_\alpha = 1$. The product $rZ_{\max}$ is dimensionless. Then, we may write using (129) that

$$\alpha = \frac{rZ_{\max}}{1 + rZ_{\max}} \Rightarrow \alpha = \frac{1}{1 + 1/rZ_{\max}} \tag{133}$$

From a point of view concerning data fitting, the transformation $r = r\left(\alpha\right)$ does not change the regression procedures: determination of r immediately leads to determination of α, and *vice versa*.

Remark 13 (On the product $\frac{\alpha}{1-\alpha}t$ and its equivalence)**.** *To agree with the analyses carried out in the preceding sections, we have to mention that the product $\frac{\alpha}{1-\alpha}t$ is equivalent to $\tau = rt$ (the dimensionless time). However, in the following calculations, to elucidate the effect of the non-integer parameter α, we will do them in terms of the observation time t, i.e., by explicitly contributing the term $\frac{\alpha}{1-\alpha}$. For more detailed discussions on the meaning of $\frac{\alpha}{1-\alpha}t$ and its relation to the time scale, we refer to [65, 66].*

6.2.1. Computations: effects of the parameter α

To present how the modified logistic law is controlled by the non-integer parameter, α, we present some simulations over different ranges of variations of the argument z (there is no need, at this moment, for z to be associated with either time or something else). The plots in Figure 33 reveal how the parameter α controls the evolutions of logistic curves, symmetrical and with midpoints at $(0, 1/2)$; in general, the increase in α results in an increase in r and steeper plots approaching faster the saturation level at unity.

6.2.2. Computations:Approximations based on sigmoidal functions

Step (Heaviside) function approximation The main problem is the determination of the Hausdorff distance between two functions f and g, denoted here as d and defined as [67, 68].

$$\rho\left(f, g\right) = \max\left\{\sup_{A \in F(f)} \inf_{B \in F(g)} \left\|A - B\right\|, \sup_{B \in F(f)} \inf_{A \in F(g)} \left\|A - B\right\|\right\} \tag{134}$$

Then, $d = \rho\left(f, g\right) = \rho\left(ah_0, s_0\right)$ should satisfy the relations $0 < H < a/2$, and $a - s_0\left(H\right)$, such that

$$\frac{a - d}{d} = e^{rd}, \quad 0 < d < a/2 \tag{135}$$

where r is the logistic rate constant.

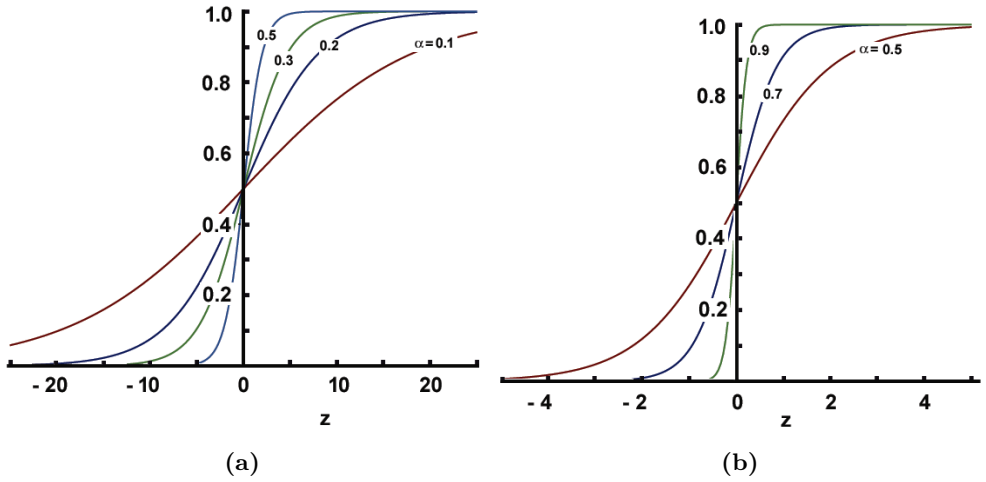

Figure 33. Plots of the logistic law (130) controlled by the non-integer parameter α: (a) For $0 < \alpha < 0.5$; (b) For $0.5 < \alpha < 1$

Following [67] (see more comments in [12]), the following non-linear equation allows us to compute the Hausdorff distance d

$$-1 + d + \frac{1}{1 + e^{-rd}} = 0 \tag{136}$$

Replacing r by $\alpha/(1-\alpha)$ we get

$$1 + d + \frac{1}{1 + e^{-\frac{\alpha}{1-\alpha}d}} = 0 \Rightarrow \frac{1}{d} ln\left(\frac{d}{1-d}\right) = -\frac{\alpha}{1-\alpha} \tag{137}$$

If the distance d is preliminary defined, then,

$$\alpha = \frac{\ln\left(\frac{d}{1-d}\right)}{\ln\left(\frac{d}{1-d}\right) - d} \tag{138}$$

Numerical solutions of (137) (by Maple) for different values of α (i.e., we stipulate the rate constant through (129)) allow us to relate the non-integer parameter and the Hausdorff distance d, as it is shown in Figure 34.

The plots in Figure 34 reveal a strong decrease in Hausdorff distance as the parameter α increases: the first 3 plots ((a), (b), and (c)) demonstrate the decrease in the Hausdorff distance as a function of α over 3 ranges, while the panel (d) shows the inverse function $\alpha = f(d)$. The results in panel (d) are in agreement with results in [67] (Table 2 in this work), where for $d = 0.00497$, the rate constant is $r = 1000$, which corresponds to $\alpha = 0.999$; the same for $r = 100$ with $d = 0.0305$, we get $\alpha = 0.991$; a distance of about $d = 0.000698$ corresponds to $r = 10000$ and $\alpha = 0.9999039$. Thus, the accuracy of approximation is easily controlled by α.

6.3. Mittag-Leffler function of one parameter in Atangana-Baleanu (AB-ML) formulation

Now, we will explore another versions of the Mittag-Leffler function of one parameter in the so-called Atangana-Baleanu formulation. Simply, this can be explained by $E_\alpha(rt^\alpha)$, with $r = \pm\frac{\alpha}{1-\alpha}$, where $(+)$ corresponds to $E_\alpha(rt^\alpha)$, while $(-)$ corresponds to $E_\alpha(-rt^\alpha)$.

Note 1: The original Atangana-Baleanu formulation corresponds to $E_\alpha(-rt^\alpha)$. Here we introduce a growing version with a positive $\frac{\alpha}{1-\alpha}$. The relationships between r and $\frac{\alpha}{1-\alpha}$ are the same as those explained in Section 6.2.

Note 2: Since the rate constant now is $\frac{\alpha}{1-\alpha}$, which is dimensionless, the argument is the observation time t.

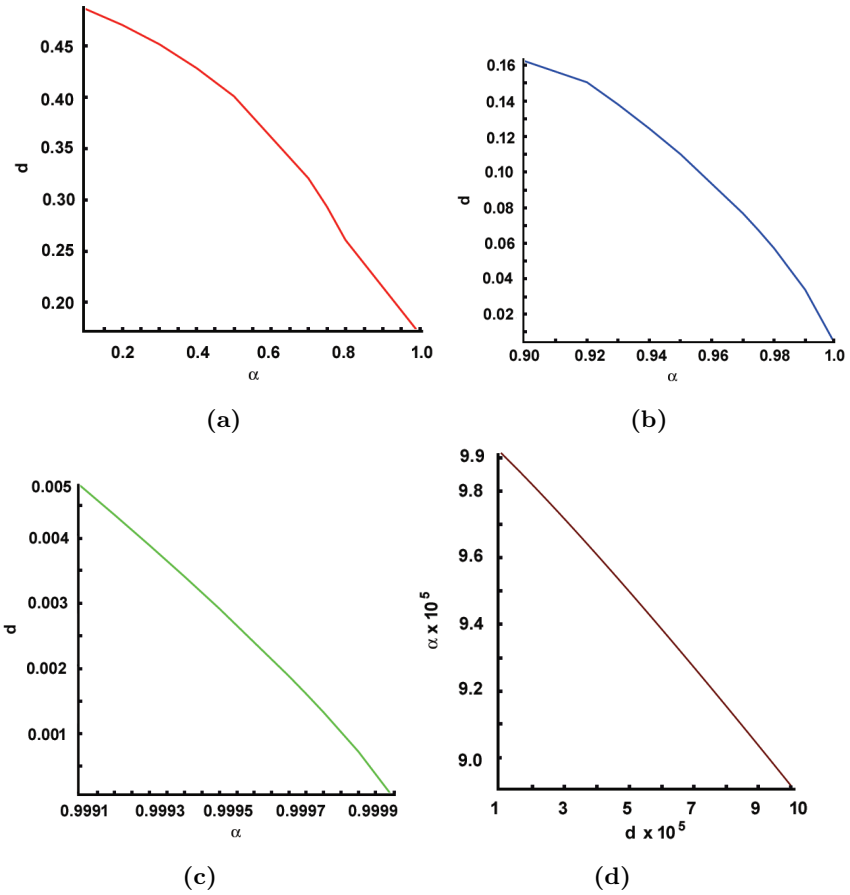

Figure 34. Plots of the Hausdorff distance controlled by the non-integer parameter α: (a) For $0.1 < \alpha < 0.9$; (b) For $0.991 < \alpha < 0.999$; (c) For $0.999 < \alpha < 0.99999$; (d)The parameter α as function of the Hausdorff distance.

6.3.1. Logistic-type law with $F(t)$ as a function of a decaying AB-ML function

Let us consider the logistic construction with $F(\tau) = {}^{AB}E_{\alpha}(-t^{\alpha})$, where $\tau = \frac{\alpha}{1-\alpha}t$, namely

$$ {}^{AB}Y_{ML-AB}(-t^{\alpha}) = \frac{1}{1 + {}^{AB}E_{\alpha}(-t^{\alpha})}, \quad 0 < \alpha < 1, \quad t \geq 0 \tag{139}$$

and we have: ${}^{AB}Y_{ML-AB}(0) = 1/2$, and ${}^{AB}Y_{ML-AB}(\infty) = 1$.
Hence, ${}^{AB}Y_{ML-AB}(-\tau^{\alpha})$ is a logistic-type function for all $t \geq 0$. Their calculations with Maple are shown in Figure 35 and require at least 400 terms to attain stable plots, and their calculations for low values of α are very sensitive when $\alpha < 0.5$ (we already discussed similar computational effects in Section 3.2.1).

6.3.2. $F(t)$ as a function of a growing AB-ML function

To construct a logistic-type function with a growing, ${}^{AB}E_{\alpha}(t^{\alpha})$, we suggest $F(t) = 1/E_{\alpha}(t^{\alpha})$, namely

$$ {}^{AB}Y_{ML-AB}(t^{\alpha}) = \frac{1}{1 + \frac{1}{{}^{AB}E_{\alpha}(t^{\alpha})}}, \quad 0 < \alpha < 1, \quad t \geq 0 \tag{140}$$

In this case $F(0) = 1/E_{\alpha}(0) = 1$ and ${}^{AB}Y_{ML-AB}(0) = 1/2$, $F(\infty) = 1/E_{\alpha}(\infty) = 0$ and ${}^{AB}Y_{ML-AB}(\infty) = 1$. The construction (140) can be obtained through the sigmoidal transformation with $x = {}^{AB}E_{\alpha}(\tau^{\alpha})$, that is

$$ {}^{AB}Y_{ML-AB}(t^{\alpha}) = \frac{{}^{AB}E_{\alpha}(\tau^{\alpha})}{1 + {}^{AB}E_{\alpha}(\tau^{\alpha})} = \frac{1}{1 + \frac{1}{{}^{AB}E_{\alpha}(t^{\alpha})}}, \quad 0 < \alpha < 1, \quad t \geq 0 \tag{141}$$

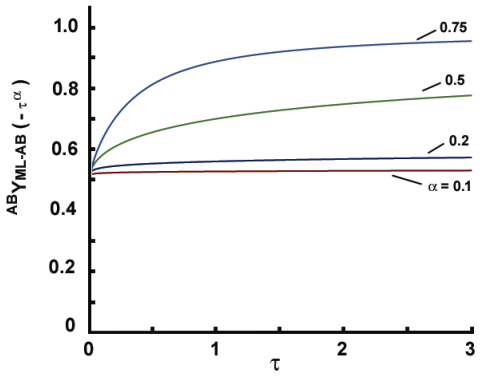

(a)

Figure 35. Logistic function with ${}^{AB}E_{\alpha}(-t^{\alpha})$ created by (139): Computations by Maple with a series of 550 terms.

The computations by Maple are stable and need at least 5-10 terms to create the plots shown in Figure 36.

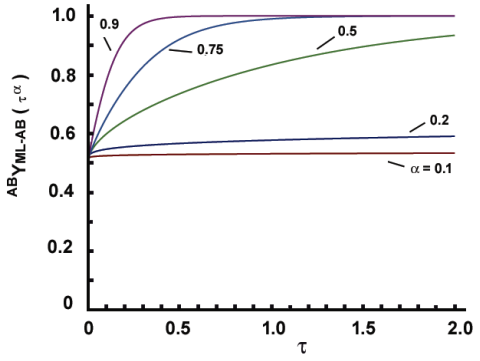

(a)

Figure 36. Logistic function with ${}^{AB}E_{\alpha}(t^{\alpha})$ created by (140): Computations by Maple with a series of 10 terms

6.3.3. Logistic law with $F(t)$ defined by Lambert transform involving ${}^{AB}E_{\alpha}(t^{\alpha})$

Following the already explored idea to create $F(\tau)$ by a Lambert transform involving the Mittag-Leffler function (see Section 5.3.2), we suggest now the construction

$$F(t) = \frac{1}{{}^{AB}E_{\alpha}(t^{\alpha}) - 1}, \quad 0 < \alpha < 1, \quad t \geq 0 \tag{142}$$

which is unbounded at the origin, i.e., $F(0) \to \infty$, but $F(\infty) \to 0$ (see the plots in Figure 37-panel (a). The resultant logistic-type law is

$${}^{AB}Y^{L}_{ML-AB}(t) = \frac{1}{1 + \frac{1}{{}^{AB}E_{\alpha}(t^{\alpha}) - 1}}, \quad 0 < \alpha < 1, \quad t \geq 0 \tag{143}$$

and ${}^{AB}Y^{L}_{ML-AB}(0) = 0$, ${}^{AB}Y^{L}_{ML-AB}(\infty) = 1$.

Hence, we have a logistic-type function starting at the origin (see Figure 37-panel (b). The calculations by Maple are stable and require at least 5-10 terms. The corresponding calculations were done by Mathematica and are shown in Figure 37-panel (c).

The construction (143) can be obtained directly through the sigmoidal transformation

$${}^{AB}Y^{L}_{ML-AB}(t^{\alpha}) = \frac{{}^{AB}E_{\alpha}(t^{\alpha}) - 1}{1 + ({}^{AB}E_{\alpha}(t^{\alpha}) - 1)} = \frac{1}{1 + \frac{1}{{}^{AB}E_{\alpha}(t^{\alpha}) - 1}}, \quad 0 < \alpha < 1, \quad t \geq 0 \tag{144}$$

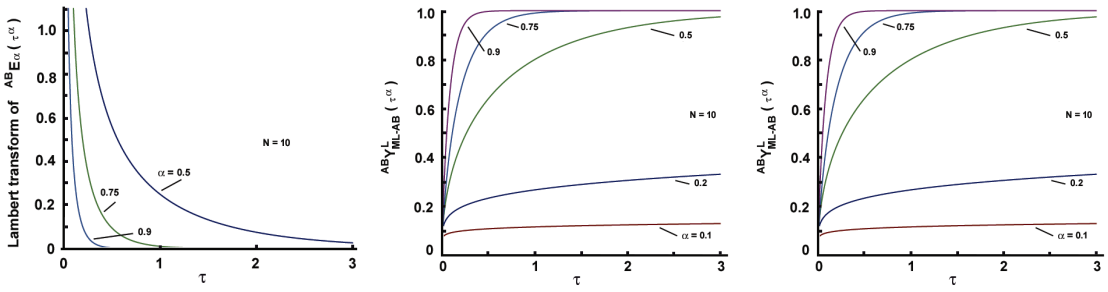

(a) **(b)** **(c)**

Figure 37. Logistic function with ${}^{AB}E_{\alpha}(t^{\alpha})$ created by (143); (a) Computations by Maple of $F(t) = \frac{1}{{}^{AB}E_{\alpha}(t^{\alpha})-1}$ (Eq.(142)). (b) Computations by Maple (10 terms of the series). (c) Computations by Mathematica

7. Current development summaries and ideas—how about we continue the discussion?

It is reasonable at the end of this long exercise to strike a balance and see what was achieved and the problems emerging, as well as some new ideas inspired by the results developed.

7.1. Outlines of the main results

In general, it was demonstrated that sigmoids can be created by implementing Mittag-Leffler functions. The study was restricted to the applications of Mittag-Leffler functions of one and two parameters, thus making the exposition clearer and easily understandable. We especially avoided the use of the three-parameter Mittag-Leffler function and the Prabhakar kernel since the increase in the number of parameters controlling the functions would make the demonstration of the approach developed complicated, but this is still an unexplored trend. The examples provided reveal that we can create either sigmoids in the sense of Verhulst, that is, with midpoints at $(0, 1/2\,)$ or S-shaped functions starting at $(0, 0)$, all of them approaching unity at infinity, in fact, at high values of the argument. The approach to use the dimensionless time τ instead of the product rt allows us to present the results in a common style and easily compare them. It was demonstrated by applying the Lambert transform that sigmoids can be created by using functions that substitute the classical exponential, which are either bounded or unbounded at the origin. Last but not least, the Mittag-Leffler function in the Atangana-Baleanu sense was also used to create sigmoids controlled by a non-integer parameter.

7.2. Main computational problems

The main computational problems emerging when Maple and Mathematica are used can be outlined as : Maple is more flexible and easier to create formulations in contrast to the complicated syntax of Mathematica. However, when the number of terms in the series of the Mittag-Leffler function increases, or the argument $\tau$is large, there are problems with the stability of the computations, as we reported. In general, the computations of the Mittag-Leffler function by series are strongly challenging problems when we have to work with $E_{\alpha}(-\tau^{\alpha})$. However, working $E_{\alpha}(\tau^{\alpha})$ on such computational problems was not addressed in this work. We especially avoided any other methods to calculate the Mittag-Leffler function, such as those discussed in [34, 69–76] since the main idea was to demonstrate the possibilities and the outcomes of the main idea. However, further works draw attention to this problem, parallel to the data fitting [77–80] when experimental results are available.

8. Final comments

As the main outcome of this study, we may outline the possibility of creating sigmoids on the basis of Mittag-Leffler functions. Many versions are possible when specific cases are considered.

The readers can recognize different issues in the presented results and apply them in various aspects, depending on the areas where they work. Thus, the first line was drawn, and I hope that this is not the last one, inspired by the ideas behind this work.

9. Appendices

9.1. Appendix A: Classical logistic model and a solution

Consider the classical logistic differential equation, with a carrying capacity K, in a form available in many textbooks

$$\frac{dy}{dt} = -ry\left(1 - \frac{p}{K}\right) \tag{145}$$

It has a popular solution developed through the separation of variables, starting with the rearrangement as

$$\frac{dy}{y\left(1 - \frac{y}{K}\right)} = rt \Rightarrow \frac{1}{y} + \frac{1}{K - y} = rt \tag{146}$$

Then, the integration of (146) yields

$$ln\frac{y}{K - y} = rt + C \Rightarrow \frac{y}{K - y} = e^{-rt-C} \Rightarrow y(t) = \frac{y_0 K e^{rt}}{(K - y_0) + y_0 e^{rt}} \tag{147}$$

or as

$$y = \frac{K}{1 + Ae^{-rt}}, \quad A = \frac{K - y_0}{y_0} \tag{148}$$

Setting $d^2y/dt^2 \ = 0$, we get the inflection point $t = \frac{1}{r}\ln\frac{K-y_0}{y_0}$. However, if $y_0 > K$, the curve has no inflection point .

9.2. Appendix B: Fractional operators and Mittag-Leffler type Functions

9.2.1. Time-fractional operators with singular (power-law) memory

We start with same definitions which will be useful in reading the following text even though they are available in many texts devoted to fractional modeling and textbooks [82]

Fractional integral: The Riemann-Liouville fractional integral of order $\alpha > 0$ is a natural result of the Cauchy multiple integral the m-fold primitive of a function $f(t)$ expressed as a single integral convolution for arbitrary positive number $\alpha > 0$ [81, 82]

$${}_0I^{\gamma} f(t) = \frac{1}{\Gamma(\gamma)} \int_0^t (t - z)^{\gamma-1} f(z) dz, \quad t > 0, \quad n \in \mathbf{R}^+ \tag{149}$$

with a law of exponents: ${}_0D^{-\gamma}{}_0D^{-\alpha} f(t) =_0 D^{-\gamma-\alpha} f(t) =_0 D^{-\gamma}{}_0D^{-\alpha} f(t)$ where $LT\left[R(s) > 0\right]$, and $F(s) = LT\left[f(t)\right]$ are Laplace transforms.

Riemann-Liouville time-fractional derivative: The Riemann-Liouville time-fractional derivative is defined as [81, 82]

$${}_0D^{\gamma} f(t) =_0 D^m{}_0I^{m-\gamma} f(t) = \frac{1}{\Gamma(m - \gamma)} \frac{d^m}{dt^m} \int_0^t \frac{f(z)}{(t - z)^{\gamma+1-m}} dz, \quad m - 1 < \gamma < m, \quad m \in \mathbf{N} \tag{150}$$

The fractional Riemann-Liouville of constant C is not zero and is a decaying power function, namely

$${}^{RL}D_t^{\alpha} C = C\frac{t^{-\alpha}}{\Gamma(1 - \alpha)} \tag{151}$$

Caputo time-fractional derivative: The Caputo derivative of a casual function $f(t)$ is defined [82–84] as

$$ {}^{C}D_t^{\alpha} f(t) =_0 I^{m-\alpha} \frac{d^m}{t^m} f(t) =_0 D_t^{-(m-\alpha)} f^{(m)} = \frac{1}{\Gamma(m-\alpha)} \int_0^t \frac{f^{(m)}(z)}{(t-z)^{\alpha+1-m}} dz, \quad m-1 < \alpha < m \tag{152} $$

For $m = 1$ we have the common definition

$$ {}^{C}D_t^{\alpha} f(t) = \frac{1}{\Gamma(1-\alpha)} \int_0^t \frac{1}{(t-s)^{\alpha}} \frac{df(s)}{ds} ds \tag{153} $$

It is clear that Caputo derivative of a constant is zero. Further, when $f(0) = f'(0) = f''(0) = ... = f^{(n)}(0) = 0$, then the Riemann-Liouville and the Caputo derivatives coincide.

9.2.2. One-parameters Mittag-Leffler function

The Mittag-Leffler function is defined as a power-series convergent in the whole complex plane [85, 87]

$$ E_{\lambda\alpha}(t) = \sum_{k=0}^{\infty} \frac{(\lambda t)^{k\alpha}}{\Gamma(\alpha k + 1)}, \quad E_{\alpha}(-\lambda t^{\alpha}) = \sum_{k=0}^{\infty} \frac{(-1)^k (\lambda t)^{\alpha k}}{\Gamma(\alpha k + 1)}, \quad 0 < \alpha < 1, \quad t > 0 \tag{154} $$

and is an entire function of order $1/\alpha$; it is a completely monotone (CM) function [85] that implies $(-1)^m \frac{d^m}{dz^m} E_{\alpha}(z) \geq 0$.

For $t \to 0^+$, and assuming $\lambda = 1$, the asymptotic expansion matches the stretched exponential [85]

$$ E_{\alpha}(-t^{\alpha}) = 1 - \frac{t^{\alpha}}{\Gamma(\alpha+1)} + \cdots \sim \exp\left[-\frac{t^{\alpha}}{\Gamma(\alpha+1)}\right], \quad t > 0 \tag{155} $$

while for $t \to \infty$ the asymptote is a negative power-law $\equiv t^{-\alpha}$ [85]

$$ E_{\alpha}(-t^{\alpha}) \approx \sum_{k=0}^{\infty} (-1)^{k-1} \frac{t^{-\alpha k}}{\Gamma(1-\alpha k)}, \quad t \to \infty \tag{156} $$

and as a first order approximation we have [85]

$$ E_{\alpha}(-t^{\alpha}) \sim \frac{t^{-\alpha}}{\Gamma(1-\alpha)} = \frac{sin(\alpha\pi)}{\pi} \frac{\Gamma(\alpha)}{t^{\alpha}}, \quad t \to \infty \tag{157} $$

9.2.3. Two-Parameters Mittag-Leffler Function

The two-parameter of the Mittag-Leffler type is defined as a series expansion

$$ E_{\alpha,\beta}(\lambda z) = \sum_{k=0}^{\infty} \frac{(\lambda z)^k}{\Gamma(\alpha k + \beta)}, \quad z \in \mathbb{C}, \quad \alpha > 0, \quad \beta > 0, \quad \beta \in \mathbb{C} \tag{158} $$

For $\beta = 1$ we get the classical one-parameter Mittag-Leffler function $E_{\alpha,1}(z)$ defined by (154)

From the definitions (154) and (158) it follows that [85, 87, 88]

$$ E_{1,1}(\lambda z) = \sum_{k=0}^{\infty} \frac{(\lambda z)^k}{\Gamma(k+1)} = \sum_{k=0}^{\infty} \frac{z^k}{k!} = e^{\lambda z} \tag{159} $$

$$ E_{1,2} = \sum_{k=0}^{\infty} \frac{z^k}{\Gamma(k+2)} = \sum_{k=0}^{\infty} \frac{z^k}{(k+1)!} = \frac{1}{z} \sum_{k=0}^{\infty} \frac{z^{k+1}}{(k+1)} = \frac{e^z - 1}{z} \tag{160} $$

The corresponding Laplace transforms are [85, 87, 88]

$$ \mathcal{L}\left[t^{\beta-1} E_{\alpha,\beta}(-\lambda t^{\alpha})\right] = \frac{s^{\alpha-\beta}}{s^{\alpha} + \lambda} = \frac{s^{-\beta}}{1 + \lambda s^{-\alpha}} \tag{161} $$

$$ \mathcal{L}\left[t^{\alpha k+\beta-1} E_{\alpha,\beta}^{(k)}(-\lambda t^{\alpha})\right] = \frac{k! s^{\alpha-\beta}}{(s^{\alpha} - \lambda)^{k+1}}, \quad k = 0, 1, 2, \ldots \tag{162} $$

$E_{\gamma,\beta}(-z)$ is completely monotonic [81, 82, 85, 87, 88] for any $\gamma \in (0,1]$, precisely if and only if $\gamma \in (0,1]$ and $\beta \geq \gamma$.

The Riemann-Liouville fractional derivative to (158) yields [81, 88]

$$ {}_0D_t^{\mu}\left[t^{\gamma k+\beta-1}E_{\gamma,\beta}^{(k)}(\lambda t^{\gamma})\right] = t^{\gamma k+\beta-\mu-1}E_{\gamma,\beta-\mu}^{(k)}(\lambda t^{\gamma}) \tag{163} $$

When, $k=0$, $\lambda=1$ and $\mu=m$ is an integer we get [88]

$$ \frac{d^m}{dt^m}\left[t^{\beta-1}E_{\gamma,\beta}(t^{\gamma})\right] = t^{\beta-m-1}E_{\gamma,\beta-m}(t^{\gamma}), \quad m=1,2,3,..... \tag{164} $$

For $m=1$ we have

$$ \frac{d}{dt}\left[t^{\beta-1}E_{\gamma,\beta}(t^{\gamma})\right] = t^{\beta-2}E_{\gamma,\beta-1}(t^{\gamma}) \tag{165} $$

When $\beta=1$ (one parameter Mittag-Leffler function), then (165) reduces to

$$ \frac{d}{dt}\left[E_{\gamma,1}(t^{\gamma})\right] = \frac{E_{\gamma,0}(t^{\gamma})}{t} \tag{166} $$

In this context, the first derivative of $E_{\gamma}(-t^{\gamma})$ and the first derivative of $E_{\gamma,\beta}(-t^{\gamma})$ are related as follows [82]

$$ \frac{d}{dt}\left[E_{\gamma,\gamma}(-t^{\gamma})\right] = t^{-(1-\gamma)}E_{\gamma,\gamma}(-t^{\gamma}) = -\frac{d}{dt}E_{\gamma}(-t^{\gamma}) \tag{167} $$

For $\lambda \neq 1$ we have [88]

$$ \frac{d}{dt}\left[E_{\gamma,1}(\lambda t^{\gamma})\right] = \frac{E_{\gamma,0}(\lambda t^{\gamma})}{t}, \quad \int_0^t \frac{d}{dt}\left[E_{\gamma,1}(\lambda t^{\gamma})\right] = \frac{E_{\gamma,0}(\lambda t^{\gamma})}{t} \tag{168} $$

That is

$$ \int_0^t \frac{d}{dt}\left[E_{\gamma,1}(\lambda t^{\gamma})\right] = \frac{E_{\gamma,0}(\lambda t^{\gamma})}{t} \tag{169} $$

Following Mainardi [32] the Mittag-Leffler function of two parameters converges at infinity to exponential function $t^{-\alpha k}$ while for the asymptotic behavior art the origin we have a starched exponential (see also [86]), precisely

$$ E_{\alpha,\beta}(-t^{\alpha}) \approx \exp\left[-\frac{t^{\alpha}}{\Gamma(\alpha+\beta)}\right], \quad t \to 0 \tag{170} $$

$$ E_{\alpha,\beta}(-t^{\alpha}) \approx \sum_{k=1}^{\infty}(-1)^{k-1}\frac{t^{-\alpha k}}{\Gamma(\beta-\alpha k)}, \quad t \to \infty \tag{171} $$

9.3. Distributions related to the Mittag-Leffler function

In general, the Mittag-Leffler function $E_{\alpha}(-x^{\alpha})$, is completely monotonic function, but it is not a statistical distribution [36, 37]. A statistical cumulative distribution represented through the Mittag-Leffler has been introduced by Pillai [36, 37] as

$$ G_x^{\alpha} = 1 - E_{\alpha}(-x^{\alpha}) = \sum_{k=1}^{\infty}\frac{(-1)^{k+1}x^{\alpha k}}{\Gamma(1+\alpha k)}, \quad 0<\alpha<1, \quad x \geq 0 \tag{172} $$

where $G_x(x)=0$ for $x \leq 0$.

The density function $g_x^{\alpha}(x) = dG_x^{\alpha}(x)/dx$ is [36, 37]

$$ g_x^{\alpha} = \sum_{k=1}^{\infty}\frac{(-1)^{k+1}x^{\alpha k}}{\Gamma(\alpha k)} = \sum_{k=0}^{\infty}\frac{(-1)^{k+1}x^{\alpha+\alpha k}}{\Gamma(\alpha+\alpha k)}, \quad 0<\alpha\leq 1, \quad x \geq 0 \tag{173} $$

If k is replaced by $k+1$, then

$$ g_x^{\alpha} = x^{\alpha-1}E_{\alpha,\alpha}(-x^{\alpha}), \quad 0<\alpha\leq 1, \quad x \geq 0 \tag{174} $$

The Laplace transform of the density (174) is [36, 37]

$$\mathcal{L}\left[E_{\alpha,\alpha}\left(x\right)\right]=\int_{0}^{\infty}e^{-sx}x^{\alpha-1}E_{\alpha,\alpha}\left(-x^{\alpha}\right)ds=\frac{1}{1+s^{\alpha}}=f_{\alpha}\left(s\right),\quad\left|s^{\alpha}\right|<1 \tag{175}$$

where $f_{\alpha}\left(s\right)$ is completely monotone (and $f_{\alpha}\left(0\right)=1$) and therefore it is a probability distribution function [36].

The Mittag-Leffler distribution is associated with the Mittag-Leffler process $X_{\alpha}\left(t\right)$, $t>0$ [36, 39, 40] where the Laplace transform is $\mathcal{L}\left[X_{\alpha}\left(t\right)\right]=\frac{1}{1+s^{\alpha}}$, $s>0$, and it obeys the following distribution [38]

$$G_{t}^{\alpha}\left(x\right)=\sum_{k=0}^{\infty}\left(-1\right)^{k}\frac{\Gamma\left(t+k\right)x^{\alpha(t+k)}}{k!\Gamma\left(t\right)\Gamma\left(1+\alpha\left(t+k\right)\right)},\quad x>0 \tag{176}$$

For $t=1$, then, $G_{t}^{\alpha}\left(x\right)$ reduces to $G_{x}^{\alpha}\left(x\right)$, as well as for $\alpha=1$, i.e., $G_{1}^{1}\left(x\right)$ recovers the Gamma distribution [38].

9.4. Appendix C: Another candidate function-Properties

9.4.1. Lambert kernel function

The Lambert function appears as a singular kernel $\frac{1}{e^{\alpha t}-1}$ in the Lambert transform $\left(\mathcal{W}_{\mathcal{L}}\left[f(t)\right]\right)$ for some suitable functions $f\left(t\right)$ [44], namely

$$\mathcal{W}_{\mathcal{LS}}\left[f(t)\right]\Rightarrow F\left(\alpha\right)=\int_{0}^{\infty}f\left(t\right)\frac{1}{e^{\alpha t}-1}dt,\quad x>0 \tag{177}$$

In 1958, Goldberg [47] considered transforms with a kernel expressed as (see also [48])

$$\frac{1}{e^{\alpha t}-1}\approx\sum_{k=1}^{\infty}b_{k}e^{-k\alpha t}dt,\quad\alpha>0 \tag{178}$$

where b_{k} is a fairly general class of real numbers.

Following Widder [44], the Lambert function can be presented as a series

$$\sum_{k=1}^{\infty}\frac{b_{k}\alpha^{k}}{1-\alpha^{k}} \tag{179}$$

and the integral analog of the transform is [44]

$$F\left(\alpha\right)=\int_{0}^{\infty}\frac{b(t)}{e^{\alpha t}-1}dt\Rightarrow F\left(\alpha\right)=\int_{0}^{\infty}\frac{1}{e^{\alpha t}-1}db(t) \tag{180}$$

where the second definition is its Stieltjes version is [44],

Since the kernel is singular for $t=0$, the change of variables [44] $\alpha tb\left(t\right)=a\left(t\right)$ and $db\left(t\right)=\alpha tb\left(t\right)$ yields a continuous (non-singular) kernel ($\mathcal{W}_{\mathcal{LN}}$ denotes Lambert-Widder transform with non-singular kernel [49]) , namely

$$\frac{\alpha t}{e^{\alpha t}-1}\Rightarrow\mathcal{W}_{\mathcal{LN}}=\int_{0}^{\infty}\frac{\alpha t}{e^{\alpha t}-1}f(t)dt \tag{181}$$

The kernel is bounded because for any $\alpha>0$

$$\lim_{t\rightarrow0^{+}}\left(\frac{\alpha t}{e^{\alpha t}-1}\right)=1 \tag{182}$$

Acknowledgments

The author highly acknowledges the invitations of the editors of TCMIS to contribute to the journal and the opportunity to express his point of view on old but forever young and intriguing topics of logistic models and sigmoid functions , now developing a new trend in model constructions.

Funding

This work is developed as part of contract No: $BG - RRP - 2.004 - 0002 - C01$, project name: BiOrgaMCT, $ProcedureBG - RRP - 2.004$, Establishing of a network of research higher education institutions in Bulgaria", funded by Bulgarian National Recovery and Resilience Plan.

Conflict of interest

There is no conflict of interest to disclose.

Author contributions

Jordan Hristov is the sole author of this text, including all parts of it, starting from the concept, analysis, data collection, and interpretations, as well as graphical illustrations.

Declaration of using AI tools

The author declares that he has not used any type of generative artificial intelligence for the writing of this manuscript, nor for the creation of images, graphics, tables, or their corresponding captions.

References

[1] P. Verhulst, "Recherches mathématiques sur la loi de d'accrooissement de la population", *Nouv.Mem. Acad.R. Soc.Belle-Lettr., Bruxelles*, vol.18, pp.1-38, 1845.

[2] F.R. Oliver, "Method of estimating the logistic growth function", *J. R. Stat. Soc*, vol.13, pp.57–66, 1964. https://doi.org/10.2307/2985696.

[3] N. Balakrishnan, *Handbook of the logistic distribution*, NY:Marcel Dekker, 1992.

[4] A. Farzad, H. Mashayekhi, H. Hassanpour, "A comparative performance analysis of different activation functions in LSTM networks for classification" , *Neural Comp. Applic.*, 31, 2507–2521,2019. https://doi.org/10.1007/s00521-017-3210-6.

[5] T. Szandala, "Review and comparison of commonly used activation functions for deep neural networks", In: Bhoi, A., Mallick, P., Liu, CM., Balas, V. (eds) Bio-inspired Neurocomputing. Studies in Computational Intelligence, vol 903. Springer, Singapore. https://doi.org/10.1007/978-981-15-5495-7_11.

[6] S.R. Dubey, S.K. Singh, B.B., Chaudhuri, "Activation functions in deep learning: A comprehensive survey and benchmark", *Neurocomputing*, 503, 92-108, 2022. https://doi.org/10.1016/j.neucom.2022.06.111.

[7] A.J.Lotka, *Elements of physical biology*, Baltimor:Williams and Wilkins, 1925.

[8] J. Berny, "New concepts and applications in growth phenomena", *J. Appl. Stat.*, vol.21, pp.161-190, 1994. https://doi.org/10.1080/757583654.

[9] F.J. Richards, "A flexible growth function for empirical use", *J. Exp. Botany*, vol.10, pp.290-300,1959. http://www.jstor.org/stable/23686557.

[10] W. Feller, "On the logistic law of growth and its empirical verification in biology", *Acta Biotheor.*, vol.5, pp.51-56,1940. https://doi.org/10.1007/BF01602862.

[11] A. Tsoularis and J. Wallace, "Analysis of logistic growth models", *Math. Biosci.*, vol 179, pp.21–55, 2002. https://doi.org/10.1016/S0025-5564(02)00096-2.

[12] J. Hristov, "The logistic models and sigmoid functions: A variety of models and solution perspectives", *Transactions on Computational Modelling and Intelligent Systems*, vol.1, pp.21-55, 2025, Article 10002, https://doi.org/10.65112/tcmis.10002.

[13] M.E. Turner Jr, B.A. Blumenstein and J. L.Sebaugh, " A generalization of the logistic law of growth", *Biometrics*, vol.25, pp.577-580, 1969. https://doi.org/10.2307/2528910.

[14] M.E. Turner Jr, E.L. Bradley Jr, and K. Kirk, "A theory of growth", *Math Biosciences*, vol 29, pp.367–373, 1976. https://doi.org/10.1016/0025-5564(76)90112-7.

[15] J.A. Nelder, " The fitting of a generalization of the logistic curve", *Biometrics*, vol. 17, pp.89–110, 1961. https://doi.org/10.2307/2527498.

[16] H. Levenbach, "A generalization of the logistic growth function and its estimation", *Statistica Neederlandica*, vol.27, pp.47–54, 1973.
[17] H. Hotelling," Differential equation subject to error, and population estimates", *J. Am.Stat. Asoc*, vo.22, pp.283–314, 1927. https://doi.org/10.2307/2276800.
[18] A.A. Blumberg, "Logistic growth rate functions", *J. Theoret. Biol.*, vol.11, pp.42–44, 1968. https://doi.org/10.1016/0022-5193(68)90058-1.
[19] P.S. Meyer, "Bi-logistic growth", *Techol.Forecast.Soc. Change*, vol.47, pp.89–102, 1994. https://doi.org/10.1016/0040-1625(94)90042-6.
[20] D. Thissen, D. Bock, H. Wainer and A.F. Roche, "Individual growth in stature: a comparison of four growth studies in the U.S.A", *Annal of Human Biology*, vol.3., pp.529–542, 1976. https://doi.org/10.1080/03014467600001791.
[21] P. Jolicoeur and J. Pontier, "Population growth and decline: a four parameter generalization of the logistic curve", *J.Theor.Biol.*, vol.141, pp.563–571, 1989. https://doi.org/10.1016/S0022-5193(89)80237-1.
[22] J.L. Fidalgo, I.M. Ortiz Rodriguez and W.K. Wong, "Design issues for population growth models", *J. Appl.Stat.*, vol.38, pp.501–512, 2011. https://doi.org/10.1080/02664760903521419.
[23] T. Modis, "Fractal aspects of natural growth", *Techol.Forecast.Soc. Change*, vol.47, pp.63–73, 1994. https://doi.org/10.1016/0040-1625(94)90040-X.
[24] R.D. Bock and D. Tissen, "Statistical problems of fitting individual growth curves", in *Human Physical Growth and Maturation: methodologies and factors*, F.E., Jonston, A.F. Roche and C. Susanne, Eds., New York and London: Plenum Press, 1980, pp. 265–290.
[25] K. Fujii, "Connection between growth/development and mathematical function", *Int. J.Sport and Health Sci.*, vol.4, pp.216–232, 2016. https://doi.org/10.5432/ijshs.4.216.
[26] R. Pearl, L.J. Reed, " A further note on the mathematical theory of population growth", *Proc.Nat. Acad. Sci. USA*, vol.8., pp.365–368, 1922. https://doi.org/10.1073/pnas.8.12.36.
[27] R. Buis, "On the generalization of the logistic law of growth", *Acta Bioteoretica*, vol.39, pp.185–195, 1991. https://doi.org/10.1007/BF00114174.
[28] M. Artzrouni, "Une nouvelle famille de courbes de croissance application à la transition démographique" , *Population (French Edition)*, vol.41, pp.497-509, 1986.
[29] G. Dattoli, R. Garra, " A note on differential equations of logistic type", *Reports in Math. Phys.*, vol.93, pp.301-311, 2024. https://doi.org/10.1016/S0034-4877(24)00039-9.
[30] G. Dattoli, Torre, " Operational methods and two variable Laguerre polynomials," *Atti.Acad. Cl. Sci. Fis. Mat.*, vol.132, pp.1-7, 1988.
[31] D.R. Cox, "The regression analysis of binary sequences", *J. Royal. Sta. Soc., Series B*, vol.20, pp.215-242, 1958.
[32] F. Mainardi , "On some properties of the Mittag-Leffler function e $E_\alpha(-t^\alpha)$, completely monotone for $t > 0$ with $0 < \alpha < 1$", *Discret. Contin. Dyn. Syst. Ser. B*, vol.19, pp.2267-2278, 2014. https://doi.org/10.3934/dcdsb.2014.19.2267.
[33] T. Simon, "Comparing Frechet and positive stable laws" , *Electr. J.Probab.*, vol.19, pp.1-25, 2014. https://doi.org/10.1214/EJP.v19-3058 .
[34] D. Valerio and J.T. Machado, " On the numerical computations of the Mittag-Leffler function ", *Commun. Nonlinear Sci. Simulat.*, vol.19, pp.3419-3424, 2014. https://doi.org/10.1016/j.cmsns.2014.03.014.
[35] B. Gompertz, "On the nature of the function expressive of the law of human mortality, and on a new model of determining the value of life contingencies", *Philos.Trans.R. Soc.Lond.*,vol.115, pp.513-583, 1825. https://www.jstor.org/stable/107756.
[36] R.N. Pillai, "On Mittag-Leffler functions and related distributions", *Ann.Inst. Statist. Math*, 42, pp.157-161, 1990, https://doi.org/10.1007/BF00050786.
[37] A.M. Mathai, "Some properties of Mittag-Leffler functions and matrix-variate analogues: A statistical perspective", *Frac. Calc. Appl. Anal.*, vol.13, pp.113-132, 2010.
[38] G.D. Lin, "On the Mittag-Leffler distributions", *J. Stats. Planing Inference*, vol.74, pp.1-9, 1998. https://doi.org/10.1016/S0378-3758(98)00096-2

[39] K. Jayakumar and R.N. Pillai, "The first-order autoregressive Mittag-Leffler process", *J. Appl. Prob.*, vol.30, pp.462-466, 1993.

[40] K. Jayakumar, "Mittag-Leffler process", *Math. Comp. Modell.*, vol.37, pp.1427-1434, 2003. https://doi.org/10.1016/S0895-7177(03)90050-1

[41] S. Prossdorf and A.Rathsfeld, On the integral equation of the first kind arising from a cruciform crack problem, In: *Integral Equations and inverse problems*, V. Petkov, R.Lararov, Eds., Longman-Harlow,pp., 210-219. 1991.

[42] P.R. Johnson, Semi-sigmoidal transformation for evaluating weakly singular boundary element integrals, *Int. J.Numerng.Meth.Eng*, vol.47, pp.1709-1730, 2000. https://doi.org/10.1002/(SICI)1097-0207(20000410)47:10<1709::AID-NME852>3.0.CO;2-V.

[43] B.I. Yun, Sigmoidal-type series expansion, *ANZIAM J.*, vol.49, 3, pp.431-450, 2008. https://doi.org/10.1017/S1446181108000060.

[44] D.V. Widder, An inversion of the Lambert transform, *Math. Mag.*, vol.23, pp.171-182, 1950. https://doi.org/10.2307/3029825.

[45] R.R. Goldberg, Inversion of generalized Lambert transforms, *Duke Math. J.*, vol.25, pp.459-476, 1958. doi:10.1215/S0012-7094-58-02540-7.

[46] E.S. Kennedy, "Exponential analogues of the Lambert series", *Am. J. Math.*, vol.63, pp.443-460, 1941.https://doi.org/10.2307/2371537.

[47] R.R. Goldberg, "Inversion of generalized Lambert transforms", *Duke Math. J.*, 25, pp.459-476, 1958. https://doi.org/10.1215/S0012-7094-58-02540-7.

[48] N. Hayek, B.J. Gonzalez, E.R. Negrin, "The generalized Lambert transform on distributions of compact support", *J. Math. Anal.Appl.*, vol.275, pp.938-944, 2002. https://doi.org/10.1016/S0022-247X(02)00241-X.

[49] J. Hristov, "New perspectives of the Lambert-Widder transform: Singular non-local operators with exponential memory", *Progress in Fractional Differentiation and Applications*, vol.11, pp.547-584, 2025, https://doi.org/10.18576/pfda/110309.

[50] W. Weibull, "A statistical distribution function of wide applicability", *J. Applied Mechanics*, vol.18, pp.293-297, 1951. https://doi.org/10.1115/1.4010337.

[51] M. Avrami, "Kinetics of phase change I: General theory", *J. Chem Phys.*, vol.7, pp.1103–1112, 1939. https://doi.org/10.1063/1.1750380.

[52] M. Avrami, "Kinetics of phase change I: Transformation-time relations for random distribution of nuclei", *J. Chem Phys.*, vol.8, pp.212–224, 1940. https://doi.org/10.1063/1.1750631.

[53] M. Avrami, "Kinetics of phase change I: Granulation, phase change, and microstructure", *J. Chem Phys.*, vol.9, pp.177–184, 1941. https://doi.org/10.1063/1.1750872.

[54] W.A. Johnson, R.F. Mehl, "Reaction kinetics in processes of nucleation and growth", *Trans. Am. Inst. Mining*, vol.135, pp.416-458, 1939.

[55] A.N. Kolmogorov, "A statistical theory for the recrystallization of metals", *Reports of the USSR Academy of Sciences: Materials Series*, vol.3, pp.355—359, 1937.

[56] B. Cantor, *The equations of materials*, Oxford Univ. Press, 2020. https://doi.org/10.1093/oso/9780198851875.001.0001

[57] J. Hristov, "A note on the Johnson-Mehl-Avrami-Kolmogorov kinetic model: An Attempt aiming to introduce time non-locality", *Eng*, vol.6, 242025, https://doi.org/10.3390/eng6020024

[58] M. Caputo and M. Fabrizio, "A new definition of fractional derivative without singular kernel" *Prog. Fract. Differ. Appl.*, vol.1, pp.73-85, 2015. http://doi.org/10.12785/pfda/010201.

[59] A. Atangana and D. Baleanu, New fractional derivatives with non-local and non-singular kernel: theory and application to heat transfer model, *Thermal Sci.*, vol.20, pp.763-769, 2016. http://doi.org/10.2298/TSCI160111018A.

[60] I.A. Mirza, D. Vieru, "Fundamental solutions to advection-diffusion equation with time-fractional Caputo-Fabrizio derivative"", *Comput. Math. Appl.*, vol.73, pp.1-10, 2017. https://doi.org/10.1016/j.camwa.2016.09.026

[61] H. Yépez-Martínez, J.F. Gómez-Aguilar "A new modified definition of Caputo–Fabrizio fractional-order derivative and their applications to the Multi Step Homotopy Analysis Method (MHAM)", *Journal of Comp. Appl. Math.*, vol.346, pp.247-260, 2019. https://doi.org/10.1016/j.cam.2018.07.023

[62] D. Avci and A. Yetim, "Analytical solutions to the advection-diffusion equation with the Atangana-Baleanu derivative over a finite domain", *J. BAUN Inst. Sci. Technol.*, vol.20, pp.382-395, 2018. https://doi.org/10.25092/baunfbed.487074.

[63] I.A. Mirza, M.S. Akram, N.A, Shah, W. Imtiaz and J.D. Chung, "Analytical solutions to the advection-diffusion equation with Atangana-Baleanu time-fractional derivative and a concentrated loading", *Alexandria Eng. J.*, vol.60, pp.1199-1208, 2021. https://doi.org/10.1016/j.a1199-1208ej.2020.10.043.

[64] D. Avci and A., Yetim, "Analysis of advective–diffusive transport phenomena modelled via non-singular Mittag-Leffler kernel", *Mathematical Modelling of Natural Phenomena*, vol.14, 309, 2019. https://doi.org/10.1051/mmnp/2019011.

[65] J. Hristov , "The fading memory formalism with Mittag-Leffler-type kernels as a generator of non-local operators", *Appl.Sci.*, vol.13, 3065, 2023. https://doi.org/10.3390/app13053065.

[66] J. Hristov , "The integrals of fractional operators with non-singular kernels: a conceptual approach, formulations, and normalization functions", *Prog. Frac. Diff. Appl.*, vol.10, pp.627-662, 2024. https://doi.org/10.18576/pfda/100409.

[67] N. Kyurkchiev and S. Markov, "Sigmoidal functions: Some computational and modeling aspects", *Biomath Commun.*, vol.1, pp.1-19, 2014. http://dx.doi.org/10.1145/j.bmc.2015.03.81.

[68] B. Sendov, *Hausdorff Approximations*, Boston: Kluwer, 1990.

[69] M. Concezzi and R.Spigler, "Some analytical and numerical properties of the Mittag-Leffler functions", *Frac. Calc. Appl. Anal.*, vol.18, pp.64-94, 2015. https://doi.org/doi:10.1515/fca-2015-0006.

[70] K. Diethelm, N.J. Ford and A.D., Freed, "Detailed error analysis for a fractional Adams method ", *Numer. Algorithms*, vol.1, pp.31-52, 2004. https://doi.org/10.1023/B:NUMA.0000027736.85078.be.

[71] R. Gorenflo, J. Loutchko and Y. Luchko, "Computation of the Mittag-Leffler function and its derivatives", *Frac. Calc. Appl. Anal.*, vol.5, pp.491–518, 2002 .

[72] H.J. Seybold, R. Hilfer, "Numerical algorithm for calculating the generalized Mittag-Leffler function", *SIAM J. Numer.Anal.*, vol.47, pp.69–88. 2008. https://doi.org/10.1137/070700280.

[73] R. Garrappa, M. Popolizio, " Evaluation of generalized Mittag-Leffler functions on the real line, *Adv. Comp. Math.*, vol.39, pp.205–225, 2013. https://doi.org/10.1007/s10444-012-9274-z.

[74] R. Garrappa, "Numerical evaluation of two and three parameter Mittag-Leffler functions", *SIAM J. Numer. Anal.*, vol.53, pp.1350-—1369, 2015. https://doi.org/10.1137/140971191.

[75] N. Özdemir, F. Evirgen, "A dynamic system approach to quadratic programming problems with penalty method", *Bull. Malays. Math. Sci. Soc.*, vol.33, 1, pp.79-–91, 2010.

[76] F. Evirgen, N. Özdemir, " Multistage adomian decomposition method for solving NLP problems over a nonlinear fractional dynamical system", *J. Comput. Nonlinear Dynam.*, 6, 021003, 2011. https://doi.org/10.1115/1.4002393

[77] I. Podlubny, I. Petras, T. Skovranek, " Fitting experimental data using Mittag-Leffler function",in: Proc 13th Int. Carpathian Control Conf. (ICCC), 28-31 May 2012, High Tatras, Slovakia, pp.578–581, IEEE. https://doi.org/10.1109/CarpathianCC.2012.6228711.

[78] C. Fang, H. Sub and J. Gu, "Powell's method-based nonlinear least-square data fitting for the Mittag-Leffler relaxation function", *Math.Mech.Solids*, vol.22, pp.1058–1067, 2017. https://doi.org/10.1177/10812865156162.

[79] T. Skovranek, "The Mittag-Leffler Fitting of the Phillips Curve ", *Mathematics*, vol.7, 589, 2019. https://doi.org/10.3390/math7070589.

[80] P.A. Ryapolov, E.B. Postnikov, "Mittag–Leffler function as an approximant to the concentrated ferrofluid's magnetization curve", *Fractal Fract.*, 5, 147, 2021. https://doi.org/10.3390/fractalfract5040147.
[81] K.B. Oldham, J. Spanier, *The fractional Calculus*, Academic Press, New York, USA, 1974.
[82] S. Samko, A. Kilbas, O. Marichev, O., *Fractional integrals and derivatives: Theory and Applications,* Gordon and Breach Science Publishers, Amsterdam , 1993.
[83] M. Caputo, 1966 Estimates of anelastic dissipation in the Earth's torsional modes, *Annali Geofis.*, vol.19, pp.75–94, 1966. https://doi.org/10.4401/ag-5038.
[84] M. Caputo, "Linear model of dissipation whose Q is almost frequency independent-II", *Geophys. J.R. Astr. Soc.*, vol.13, pp.529–539, 1967. https://doi.org/10.1111/j.1365-246X.1967.tb02303.x.
[85] F. Mainardi, "Why the Mittag-Leffler function can be considered the queen of the fractional calculus?" *Entropy*, 22, 1359, 2020. https://doi.org/10.3390/e22121359.
[86] N.H.T. Lemes, J.P.C. dos Santos, J.P. Braga, "A generalized Mittag-Leffler function to describe nonexponential chemical effects", *Appl. Math. Modelling*, vol.40, pp.7971-7976, 2016. https://doi.org/10.1016/j.apm.2016.04.021.
[87] I. Podlubny, *Fractional Differential Equations*, Academic Press, San Diego-Boston-New York–London-Tokyo-Toronto, 1999.
[88] R. Gorenflo, A.A. Kilbas, F. Mainardi, S.V. Rogosin, *Mittag-Leffler functions, Related topics and applications*, Berlin-Heidelberg, 2014.